MARTA SOFIA VILHENA SERRANO

ROLE OF TMBIM4 ON CANCER CELL SURVIVAL AND PROLIFERATION

Supervisor: Professor Doutor Nuno Ricardo de Almeida Saraiva

Co-supervisor: Mestre Marta Filipa Malheiro Martins

Universidade Lusófona

Escola de Ciências e Tecnologias da Saúde

Lisbon

2024

MARTA SOFIA VILHENA SERRANO

ROLE OF TMBIM4 ON CANCER CELL SURVIVAL AND PROLIFERATION

VERSÃO FINAL

Tese defendida em provas públicas na Universidade Lusófona, Centro Universitário de Lisboa no dia 04/04/2024, perante o júri, nomeado pelo Despacho de Nomeação n.º: 74/2006, de 24 de março, com a seguinte composição:

Presidente: Prof. Doutor Luís Monteiro Rodrigues

Arguente: Prof.ª Doutora Ana Sofia Fernandes

Orientador: Prof. Doutor Nuno Saraiva

Este trabalho também foi orientado por Mestre Marta Martins.

Universidade Lusófona

Escola de Ciências e Tecnologias da Saúde

Lisbon

2024

Dedico esta dissertação à minha Avó Preciosa, que faleceu no decorrer do meu curso e por essa razão não terá a possibilidade de me ver tornar Mestre em Ciências Farmacêuticas. Avó, palavras nunca serão suficientes para expressar aquilo que significas para mim, nem para agradecer todo o amor que me deste ao longo da vida. Este trabalho é para ti. Tenho a certeza que atingir este marco te teria deixado imensamente feliz e orgulhosa da tua netinha.

Acknowledgments

Esta dissertação é o culminar de todo o trabalho que tive durante os últimos cinco anos e de todas as experiências por que passei no decorrer do meu Mestrado Integrado em Ciências Farmacêuticas na Escola de Ciências e Tecnologias da Saúde da Universidade Lusófona de Humanidades e Tecnologias. Como tal não posso deixar de agradecer às pessoas que mais marcaram o meu percurso e tornaram tudo isto possível, aos professores com quem me cruzei ao longo do caminho e me inspiraram, bem como à instituição CBIOS (Research Center for Biosciences & Health Technologies) por continuar a proporcionar aos estudantes a oportunidade de contactar com o mundo da investigação científica.

Queria começar por agradecer ao meu orientador, o Professor Doutor Nuno Saraiva por ter aceitado acompanhar-me nesta caminhada, que começou na unidade curricular de Projeto I, no 4º ano. Obrigada por acreditar em mim e no meu potencial, por todo o feedback, incentivo e ajuda durante esta dissertação.

Um gigante obrigada também à minha coorientadora, Doutoranda Marta Martins, com quem partilhei infindáveis horas no laboratório e que teve paciência para me explicar todos os ensaios e protocolos, e me ensinar praticamente tudo o que sei sobre cultura celular, investigação e laboratórios. Foi uma experiência incrível. Obrigada por veres o meu potencial desde o primeiro dia e por incentivares o “bichinho” da investigação que há em mim.

Aos colegas e todas as pessoas com quem partilhei as paredes do laboratório, obrigada por me acolherem tão bem e me fazerem sempre sentir incluída; um obrigada particular à Ana Júlio, Sandra Ferreira e João Vieira.

Não posso terminar sem antes agradecer a todos os meus colegas de curso, em especial aos que se tornaram grandes amigos que espero poder levar comigo para a vida: Margarida Andrade, Tiago Camelier, Cristiana Bragança, Paula Oliveira e Luís Silva. Sem a vossa companhia, apoio e amizade teria sido tudo mais triste e difícil, mas sem dúvida muito mais aborrecido. Um obrigada nunca será suficiente.

Por último, mas sem dúvida não menos importante, agradeço à minha família. Mãe e pai, obrigada por todos os esforços que fizeram para que eu chegasse até aqui, empurrões na direção certa e pelo vosso apoio, força e amor incondicional. Obrigada por me educarem na pessoa que sou hoje. Foi difícil, mas sem vocês teria sido impossível. Maninho, espero que me vejas como um exemplo daquilo que conseguimos atingir com trabalho e dedicação, agora que deste início ao teu percurso no Ensino

Superior. És uma inspiração e aprendo contigo todos os dias. Obrigada por me chamares à razão tantas e tantas vezes. Ao meu Avô Renato, o meu maior exemplo de vida: se um dia chegar aos 82 anos de idade e tiver um oitavo do impacto que tens em mim na vida dos meus netos, sei que cumpri o meu propósito. Obrigada por tudo.

Sei bem o quão privilegiada sou e a sorte que tenho por ter tanto pelo qual agradecer. Independentemente do que estiver guardado para o meu futuro, vou levar sempre os últimos cinco anos e todos os que passaram pelo meu caminho no coração. Muito obrigada!

Resumo

O glioblastoma é o cancro maligno do cérebro mais comum, tem um mau prognóstico e é frequentemente resistente à Temozolomida, o quimioterápico de primeira linha no seu tratamento há décadas. De igual forma, o osteossarcoma é um cancro ósseo raro e muito agressivo, com reduzida taxa de sobrevivência. A Transmembrane BAX Inhibitor-1 Motif-containing (TMBIM4) é uma proteína do complexo de Golgi que controla os fluxos intracelulares de Ca^{2+} bem como a resistência ao stress apoptótico, regulando assim a viabilidade e metabolismo celulares. Este trabalho teve como objetivo a avaliação do impacto da desregulação da expressão da TMBIM4 no glioma e osteossarcoma.

O silenciamento da expressão da TMBIM4 resultou na redução da motilidade das células de glioma. Adicionalmente, a viabilidade dessas células após incubação com Temozolomida foi afetada pela redução da expressão da TMBIM4. As células de osteossarcoma que sobrexpressam TMBIM4 sobrevivem mais tempo em cultura com baixa disponibilidade de nutrientes. Este efeito não é dependente do aumento de H_2O_2 que ocorre por sobrexpressão da TMBIM4. Estes resultados sustentam que a TMBIM4 tem um impacto crítico em processos celulares associados à progressão do cancro, podendo vir a ser utilizada como biomarcador tumoral ou eventualmente como alvo terapêutico.

Palavras-chave: Glioma; osteossarcoma; TMBIM4; sobrexpressão; temozolomida.

Abstract

Glioblastoma is the most common malignant brain tumour, has a poor prognosis and is frequently resistant to Temozolomide, the chemotherapeutic drug used as the first line of treatment for decades. Similarly, osteosarcoma is a rare and very aggressive bone cancer with a low survival rate. Transmembrane BAX Inhibitor-1 Motif-containing (TMBIM4) is a Golgi complex protein that controls calcium intracellular fluxes as well as resistance to apoptotic stress, regulating cellular viability and its metabolism. This work had the purpose of evaluating the impact of TMBIM4's expression dysregulation on glioma and osteosarcoma.

Silencing of TMBIM4 expression resulted in the reduction of motility of glioma cells. Additionally, the viability of glioma cells after incubation with Temozolomide was affected by the reduction of TMBIM4 expression. Osteosarcoma cells overexpressing TMBIM4 survive longer in starvation culture conditions. This effect is not dependent on the TMBIM4-dependent increase H_2O_2 of TMBIM4. These results support a critical role for TMBIM4 in cellular processes associated with cancer progression, thus it could be used clinically as a cancer biomarker or, eventually, as a therapeutic target.

Keywords: Glioma; osteosarcoma; TMBIM4; overexpression; temozolomide.

Abbreviations

3D – Three dimensional

Ang-1 – Angiopoietin 1

Ang-2 – Angiopoietin 2

ATP – Adenosine triphosphate

BBB – Blood-Brain Barrier

Ca^{2+} – Calcium

CAR-T – Chimeric antigen receptor T

CAT – Catalase

CBIOS – Research Center for Biosciences & Health Technologies

CBS – Cystathionine beta-synthase

CNS – Central Nervous System

CSCs – Cancer Stem Cells

CT – Chemotherapy

CTH – Cystathionine gamma-lyase

CTLA-4 – Anti-cytotoxic T-lymphocyte-associated protein 4

ddH2O – Double distilled water

DF – Disulfiram

DMEM – Dulbecco's Modified Eagle's Low Glucose Medium

DMSO – Dimethyl sulfoxide

EGFR – Epidermal growth factor receptor

FAMMM – Familial atypical multiple mole melanoma

FBS – Fetal Bovine Serum

GB – Glioblastoma

h – hours

H_2O_2 – Hydrogen peroxide

hGAAP – Human golgi anti-apoptotic protein

HGF – Hepatocyte Growth Factor

i3S – Instituto de Investigação e Inovação em Saúde

IC50 – Half-maximal inhibitory concentration

IDO – Indolamine 2,3-dioxygenase

IGC – Instituto Gulbenkian da Ciência

IL-8 – Interleukin 8

LGG – Low-Grade Glioma

MEM NEAA – Non-Essential Amino Acids

MGMT – O^6-methylguanine-DNA methyltransferase

MTT – 3-(4,5-dimethylthiazol-2-yl)-2,5-diphenyltetrazolium bromide

N^3-MA – N^3-methyladenine

N^7-MG – N^7-methylguanine

NAC – N-Acetyl-L-Cysteine

NF1 – Neurofibromatosis type 1

NK – Natural killer

NPs – Nanoparticles

NSCs – Neural Stem Cells

O_2 – Oxygen

O^6-MG – O^6-methylguanine

OS – Osteosarcoma

OvS – Overall survival

pcDNA – Plasmid DNA

PDGFR – Platelet-derived growth factor receptor

PD-L1 – Anti-programmed cell death protein 1

PEN-STREP – Penicillin-Streptomycin Antibiotic

PFS – Progression-free survival

PI – Propidium iodide

PTEN – Phosphatase and Tensin Homolog Deleted on Chromosome Ten

RB – Retinoblastoma

ROS – Reactive oxygen species

RT – Radiotherapy

RTKs – Receptor Tyrosine Kinase

SD – Standard deviation

SEM – Standard error of the mean

SOCE – Store-operated Ca^{2+} entry

TAM - Tumour-associated macrophages

tdTomato – Tandem dimer Tomato

TMBIM – Transmembrane BAX Inhibitor-1 Motif-containing

TMZ - Temozolomide

TTF – Tumour-treating fields

USA – United States of America

VEGF – Vascular Endothelial Growth Factor

WHO – World Health Organization

WS – Working solution

Table index

Figure index

Contents

Chapter I - Introduction

Glioma

Overview, prevalence, and incidence

Figure 1 shows the most recent incidence data for brain and central nervous system (CNS) cancer according to GLOBOCAN and the World Health Organization (WHO). This group of cancers was more prevalently reported in United States of America (USA), Canada, Australia and in most European countries in 2020, with a rate of 5.2 or above per 100 000 habitants (WHO, 2023). Regarding mortality (figure 2), death from this disease was more frequent in Brazil, Portugal, France, and some other countries in Europe (WHO, 2023).

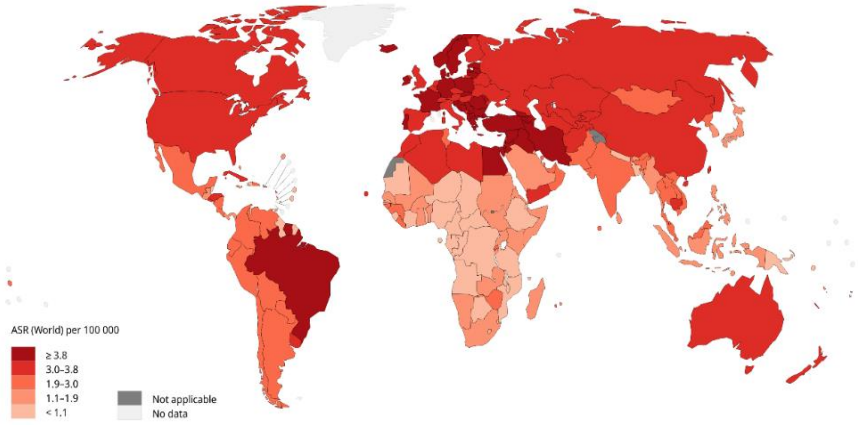

Figure 1 *– The estimated rate of age-standardized world incidence in both sexes in 2020 for brain and CNS cancer* (WHO, 2023).

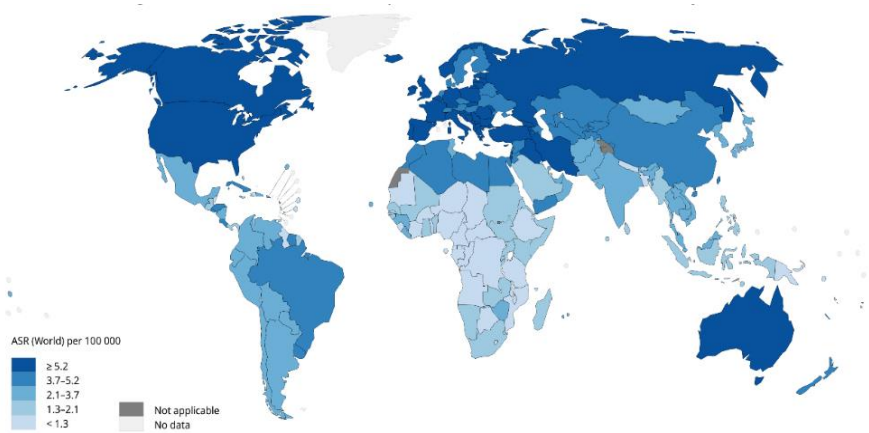

Figure 2 *– Estimated mortality rate from brain and CNS cancer worldwide in 2020 for both sexes* (WHO, 2023).

The number of brain and CNS cancer cases is predicted by the WHO to increase by 41.4 % and 41.2 % in males and females, respectively, of all age groups by 2040. In absolute values, this means that male cancer cases will go up from approximately 168 000 to 238 000 cases per year and female cases from around 140 000 to 197 000, as seen in figure 3 (WHO, 2023). As presented in figure 4, this problem is even more evident when predicted data of deaths from brain and CNS cancer is analysed, as in 2040 it is estimated that yearly losses in both male and female patients will increase over 46 % (WHO, 2023). Briefly, this data shows that although there is a clear rising tendency in both genres, these tumours are more frequent in the male population than in women. Statistics also reveal that Caucasians are more commonly affected when compared to other races (Davis, 2018; WHO, 2023).

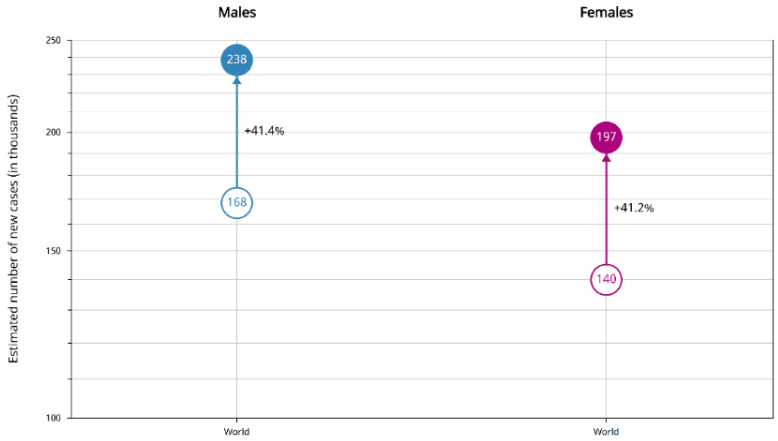

Figure 3 *– Estimated number of new brain and CNS cancer cases in the world from 2020 to 2040 in males and females of all age groups* (WHO, 2023).

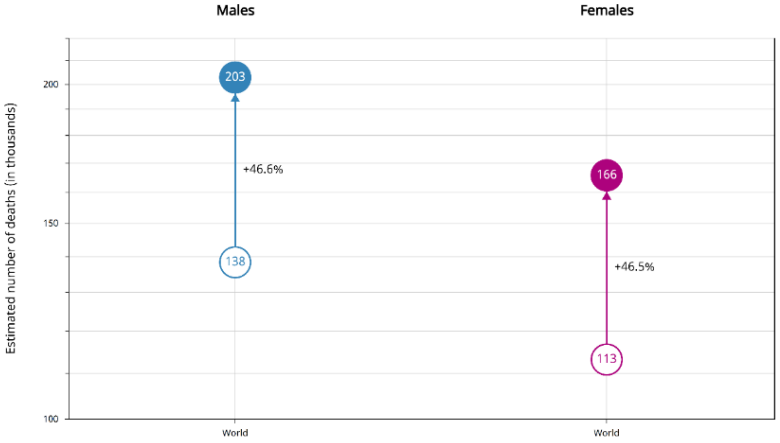

Figure 4 *– Estimated number of deaths worldwide from 2020 to 2040 in both males and females of all ages from brain and CNS cancer* (WHO, 2023).

Brain and CNS cancer is a very large and heterogenous group of tumours at a histological level, with a large impact in our current society, as mentioned above (Davis, 2018). Out of these, 81 % are gliomas, a type of tumour emerging from glial cells, the most common cells in the CNS. Glial cells have important functions such as providing oxygen and other nutrients to neurons; and can give rise to either astrocytoma, oligodendroglioma, ependymoma, or oligoastrocytoma (Davis, 2018; Xu et al., 2020). Gliomas are also classified considering the presence or absence of isocitrate dehydrogenase (IDH) and H3F3K27M mutations, 1p/19q co-deletion and ATRX loss, which is a marker of the astrocytoma lineage (Delgado-López et al., 2020). Malignant gliomas include glioblastoma (GB), anaplastic astrocytoma and anaplastic oligodendroglioma and, according to the WHO, their malignancy progresses increasingly from grade I to IV (R. Chen et al., 2017; Liu et al., 2021; Xu et al., 2020). A schematic view of this classification process can be seen below in figure 5. GB is the most common out of the CNS malignant tumours, accounting for approximately 45 % of all gliomas; the most malignant, as only 5 % of patients survive more than 5 years with this diagnosis; and the most resistant to Temozolomide (TMZ), which is the main chemotherapeutic agent used to treat these patients (Gusyatiner & Hegi, 2018; Liu et al., 2021; Ma et al., 2021; Ostrom et al., 2014; Xu et al., 2020). Symptoms of GB include headaches, seizures, and focal neurologic deficits (Liu et al., 2021).

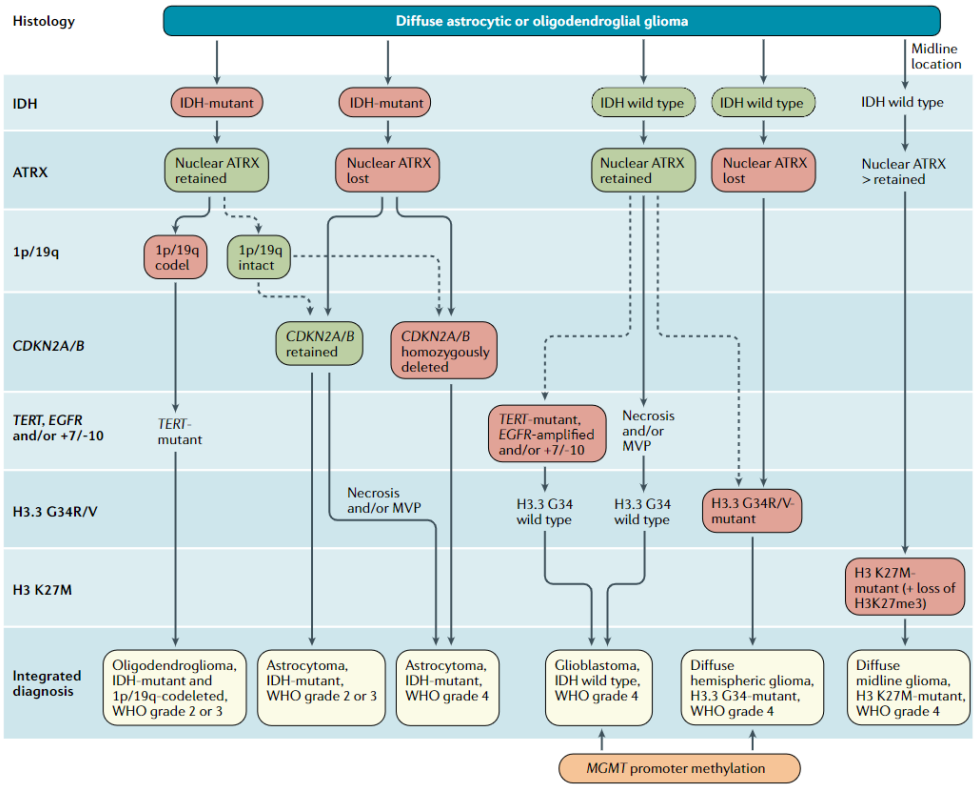

Figure 5 – *Diagram of the glioma classification process* (Weller et al., 2021).

Prognostic and challenges

Currently, life expectancy regarding glioma has a very wide range as 47 % of patients with low-grade glioma (LGG), meaning grades I and II, are expected to live more than 10 years since diagnosis, if treated with suitable therapy. However, GB has a weak prognosis of about 14 to 15 months, setting off from the same timeframe, falling into the grade IV category due to its low survival rate and high aggressiveness (Delgado-López et al., 2020; Liu et al., 2021; Xu et al., 2020). The fact that glioma cells have a high infiltrative nature and innate resistance to cancer treatment with radio or chemotherapy (CT) is related to the lack of a better prognosis (Delgado-López et al., 2020).

Regarding GB, it presents a fast progression and frequent relapse with a very invasive nature (Liu et al., 2021). One of the reasons for GB recurrence and resistance is frequently attributed to cancer stem cells (CSCs) (Delgado-López et al., 2020). These stem cells are capable of self-renewing, potentially differentiating into various types of cells, particularly cancerous ones, and from there initiating a tumour (Delgado-López et al., 2020; NHI, 2023). CSCs are inherently resistant to TMZ, maybe even selecting subpopulations that resist this drug in case of recurrence, and, when under ionizing radiation such as radiotherapy (RT), apoptosis may be suppressed, thus promoting resistance to this therapy as well (Delgado-López et al., 2020). The other reason why this type of glioma is so difficult to treat is the high degree of tumour cell heterogeneity. This may help explain why the development of therapies specific for biomarkers of glioma was not successful yet. Additionally, the fact that the drugs to treat these tumours need to cross the blood-brain barrier (BBB) to reach the tumour, as well as remaining in contact with the malignant cells by avoiding being removed by efflux pumps whose purpose is to expel unwelcome xenobiotics from that environment, makes it even more challenging to develop (R. Chen et al., 2017; Delgado-López et al., 2020; Gusyatiner & Hegi, 2018; Liu et al., 2021; Ou et al., 2021; Xu et al., 2020). Furthermore, glioma diagnosis is hard due to the lack of methods that reach deep tissues, where these tumours often reside when the disease is more advanced and chances of survival are lower, depriving patients of eventual curative therapy (Li et al., 2022). IDH is an oncometabolite enzyme coded by the IDH1 gene. IDH mutations usually happen very early in the glioma carcinogenesis process, affecting the overall prognosis of brain tumours for the better, making it a relevant prognostic marker (Davis, 2018; Delgado-López et al., 2020; Ma et al., 2021). These mutations are more often found in younger patients and are typically associated with longer survival time and reduced aggressiveness. Meaning GB IDH1 mutated tumour patients have a three-time greater survival expectancy than wildtype IDH2 (Davis, 2018; Delgado-López et al., 2020; Ma et al., 2021).

Mechanisms of carcinogenesis

Although there is not a clear etiological pathway identified to glioma, some situations and events are known to be related to its emergence (Delgado-López et al., 2020). That is the case of various rare genetic syndromes inherited through the family, such as Neurofibromatosis type 1 (NF1) and 2, Tuberous sclerosis, and von Hipple Lindau, Li-Fraumeni, Lynch, Turcot, Gorlin, Cowden, Familial atypical multiple mole melanoma (FAMMM) syndromes, Enchondromatosis disorders (including Ollier disease and Maffucci syndrome) and Rubinstein-Taybi syndrome (Davis, 2018; Delgado-López et al., 2020). Table 1 links these syndromes to their respective affected genes. Out of all of these, NF1 is the one that is most frequently associated with tumours of the CNS, followed by Tuberous sclerosis (Davis, 2018). Li-Fraumeni syndrome is linked with many different types of cancer besides brain tumours as it is caused by a mutation on p53, which is a fundamental tumour suppressor (Davis, 2018; C. Zhang et al., 2020). This leads to cases of brain tumour arising, on average, at 25 years old in 14 % of these patients (Davis, 2018). Lynch syndrome is usually related to tumours on the colon and endometrium, but its presence raises the risk of brain cancer by four times, most cases emerging before the 30-year-old mark (Davis, 2018). These disorders are all related to alterations on proto-oncogenes or tumour suppressor genes and are inherited by an autosomal dominant pattern (Davis, 2018; Delgado-López et al., 2020). To promote carcinogenesis both alleles of the suppressor gene need to be mutated. For this reason, there are still patients who can be diagnosed with a syndrome but not have their probability of developing cancer affected (Davis, 2018; Delgado-López et al., 2020).

Table 1 *– Genetic disorders and respective involved genes associated with glioma and GB* (Davis, 2018; Delgado-López et al., 2020)

Genetic disorder	**Gene affected**
Neurofibromatosis type 1	NF1
Neurofibromatosis type 2	NF2
Tuberous sclerosis	TSC2 and TCS1
Von Hipple Lindau syndrome	VHL
Li-Fraumeni syndrome	P53
Lynch syndrome	MLH1, MSH2, MSH6, PMS2
Turcot syndrome	APC, hMLH11, hMSH2, PMS2
Gorlin syndrome	PTCH1
Cowden syndrome	PTEN

FAMMM syndrome	P16/CDKN2A
Enchondromatosis disorders	IDH1, IDH2
Rubinstein-Taybi syndrome	CREBBP

In addition to all genetic conditions described above, various risk factors can be associated with development of brain tumour. Namely, the amount of radiation each person is exposed to during childhood, both regarding medical procedures and related to the environment in which the child is growing up (Davis, 2018). The very own treatment of cancer with RT can lead to genetic damage, which for its part can contribute to the appearance of a glioma tumour (Delgado-López et al., 2020). Studies have also proven the existence of a relationship between allergic diseases such as asthma, eczema and rhinitis, and a lower probability of developing glioma later in life (Davis, 2018). The protection seems to be stronger in higher grades of glioma and is related to the frequent and somewhat constant high IgE concentrations these conditions provide (Davis, 2018).

There are three primary signalling pathways that if altered can significantly contribute to the development of GB: RB, TP53, and PTEN/NF1/RTK pathways (Delgado-López et al., 2020; Reuss et al., 2023; W. Zhang et al., 2016). The first one is related to the retinoblastoma (RB) tumour suppressor gene that codes for a protein with the same name, which controls the G1/S cell cycle checkpoint (Delgado-López et al., 2020). Consequently, mutations in the RB pathway raise mitotic activity which can eventually lead to the development of malignancy (Delgado-López et al., 2020). The p53 protein is a tumour suppressor that induces apoptosis in cases of non-fixable DNA damage during the cell cycle (Delgado-López et al., 2020). The gene that codes for this protein is *tp53* and when mutated, as seen in a majority of glioma cases, helps the cell avoid death (Delgado-López et al., 2020; Reuss et al., 2023). Cell growth in glioma is partially controlled by the last pathway as receptor tyrosine kinases (RTKs) epidermal growth factor receptor (EGFR) and platelet-derived growth factor receptor (PDGFR) promote cell growth and the tumour suppressors phosphatase and tensin homolog deleted on chromosome ten (PTEN) and NF1 modulate neural stem cells (NSCs) entry in the cell cycle (Delgado-López et al., 2020). Studies with NSCs showed that deactivation of *tp53* leads to high-grade glioma (HGG) development (Delgado-López et al., 2020; Reuss et al., 2023). Epigenetic changes in oncogenes or proto-oncogenes have also been proven relevant in glioma tumorigenesis since they can result in specific mutations that allow activation or inactivation of these genes, and consequently control cell growth and their differentiation rate (Delgado-López et al., 2020). NSCs exist inside

the brain and can turn into CSCs that later develop into cancer cells, giving rise to a glioma tumour (Delgado-López et al., 2020; Qin et al., 2023).

Current treatment and therapeutic approaches

Having in mind the challenges mentioned before, the current clinical standard for glioma care follows the classic Stupp protocol which entails surgical resection followed by treatment with TMZ and RT within a month after operation, as well as adjuvant CT, also with TMZ, for 6 to 12 courses (Liu et al., 2021; Ou et al., 2021; Xu et al., 2020). RT is done during a period of 6 weeks in 30 fractions of 60 Gy (Ma et al., 2021). TMZ is given 7 days/week in a concentration of 75 mg/m^2; maintenance phase dose of 150-200 mg/m^2 is administrated daily for 5 days every 28 days (Liu et al., 2021; Ma et al., 2021). This treatment plan has not suffered adjustments since 2005 and the 5-year survival rate did not show any progress during this time (Liu et al., 2021; Ma et al., 2021). There are other available CT regiments such as the PCV (Procarbazine, Lomustine and Vincristine), the previous first-line treatment, but it has been shown that only progression-free survival (PFS) is extended under this treatment, leaving overall survival (OvS) stagnant; however, it is still used in recurrent cases (Liu et al., 2021; Ma et al., 2021). The antiangiogenic drug Everolimus is also used in combination with RT and TMZ both concurrent and adjuvant in recent GB diagnosis, but it results in increased toxicities and no significant improvement regarding PFS (Liu et al., 2021).

The mechanism of action of TMZ consists in adding methyl groups to purines, forming three different cytotoxic molecules: O^6-methylguanine (O^6-MG), N^7-methylguanine (N^7-MG) and N^3-methyladenine (N^3-MA) (Jiapaer et al., 2018; Ortiz et al., 2020). If the O^6-methylguanine-DNA methyltransferase (MGMT) gene is active in the tumour, it codes for the enzyme MGMT that repairs the damage caused by TMZ cytotoxic molecules, allowing the tumour cell to survive (Davis, 2018; Jiapaer et al., 2018; Ortiz et al., 2020). This gene is found inactive by methylation in most LGGs, supporting the fact HGGs are more resistant to TMZ (Davis, 2018). During DNA synthesis, O^6-MG pairs with a thymine, a binding that is successively corrected by the DNA Mismatch Repair (MMR) system, leading to apoptosis, which means that loss of this system prevents cell death and gives rise to resistance (Jiapaer et al., 2018; Ortiz et al., 2020). The Base Excision Repair (BER) pathway corrects methylations caused by TMZ, encouraging GB progression (Jiapaer et al., 2018). Glioma stem cells have a high capacity for proliferation and contain active DNA repair mechanisms and efflux pumps that expel drugs, contributing to increased tumour cell survival and to tumour recurrence (Jiapaer et al.,

2018; Ortiz et al., 2020). Acquired resistance can cause epigenetic changes that increase cell survival (Ortiz et al., 2020).

Due to the poor results obtained with TMZ treatment, research for better options kept progressing, leading to the emergence of new therapies like targeted molecular therapy and immunotherapy (Liu et al., 2021; Xu et al., 2020). This latter alternative is feasible in glioma due to the existence of lymphatics in the CNS and its ability to cross the BBB, although limited efficacy has been proven this far in the ongoing clinical trials and prognosis is not yet satisfactory (Liu et al., 2021; Xu et al., 2020). Additionally, glioma has an immunosuppressive nature, and tumour cells express increased levels of immunosuppressive factors (Xu et al., 2020). Bevacizumab is a humanized monoclonal antibody which targets specifically the vascular endothelial growth factor (VEGF) since it is usually overexpressed in GB. Therefore, it is classified as an angiogenesis inhibitor approved for recurrent GB (Liu et al., 2021; Ma et al., 2021; Xu et al., 2020). Its safety and efficacy have been proven both alone and in combination with irinotecan (Xu et al., 2020). Studies showed that the use of Bevacizumab from week 4 of RT and during the subsequent 12 cycles of CT extended PFS but quality of life was precarious, hence its indication in more difficult and advanced cases (Liu et al., 2021). VEGF is one of the factors involved in the angiogenic process, as well as angiopoietin 1 and 2 (Ang-1 and Ang-2), PDGFR, interleukin 8 (IL-8) and hepatocyte growth factor (HGF) (Delgado-López et al., 2020). The development of other antiangiogenic drugs besides Bevacizumab for the treatment of GB is a smart approach since it is a common characteristic of this tumour to have significant microvascular proliferation (Delgado-López et al., 2020).

Tumour-treating fields (TTF) is a selective electromagnetic field therapy that harms cancer cells by interrupting mitosis and consequently inducing apoptosis through electric fields that alternate between low field strength and intermediate intensity frequency of 1 to 3 V/cm and 200 kHz, respectively (Liu et al., 2021; Ma et al., 2021; Ou et al., 2021; Xu et al., 2020). This technique has minor to no side effects due to its selectiveness towards proliferating cells. When those occur, they are mainly skin-related (dermatitis, cutaneous infections, allergies and/or irritation) due to the contact of the sensors with the scalp (Liu et al., 2021). TTF has the advantage of disrupting the repair process of the DNA damage caused in tumour cells by RT treatment, boosting its efficacy (Liu et al., 2021). The technique is currently approved by The Food and Drug Administration (FDA) even though it is not particularly convenient for the patient money-wise and because of the large size of the device (Liu et al., 2021; Ma et al., 2021; Ou et al., 2021). In combination with TMZ, PFS was significantly prolonged since CT provides synergetic activity to this method, but evidence regarding survival advantage is still weak

and controversial making it unavailable in Europe as more criteria need to be met (Liu et al., 2021; Ma et al., 2021).

Innovation and potential new treatment options

The future of glioma treatment depends on the development of precision medicine, meaning defining relevant biomarkers and coming up with highly bioactive and specific new drugs. However, the high heterogeneity of glioma cells makes it difficult to determine targets to specifically treat this disease (Delgado-López et al., 2020; Ou et al., 2021; Xu et al., 2020). To obtain better therapeutic outcomes, nanoparticles (NPs) have been used to convey TMZ, improving its pharmacokinetics and reducing toxicity (Ortiz et al., 2020). NPs, while having their own encounters, have the necessary characteristics to meet the needs of precision medicine, addressing the challenges of glioma treatment by being used in diagnosis to early detect the disease, being able to cross the BBB, and their morphology can be modulated accordingly to preference (Li et al., 2022).

Blockage of immune checkpoint inhibitors such as indolamine 2,3-dioxygenase (IDO), anti-cytotoxic T-lymphocyte-associated protein 4 (CTLA-4) and anti-programmed cell death protein 1 (PD-L1) has shown promising efficacy, particularly regarding PD-L1 and CTLA-4, since GB tumours usually present high expression levels of these molecules, which correlates with tumour progression (Ma et al., 2021; Xu et al., 2020). Mouse models studies done on glioma cells increased survival, but so far clinical trials with Nivolumab and Ipilimumab, anti-PD-L1 and anti-CTLA-4 monoclonal antibodies respectively, have not proven any change in OvS (Ma et al., 2021; Xu et al., 2020). IDO high expression is also linked to a worse prognosis in many cancers. Inhibition of this enzyme combined with TMZ presented great preclinical results in mice with GB but lacked in clinical trials in both PFS and OvS (Xu et al., 2020).

There are other new therapies still under refinement such as oncolytic viruses or tumour vaccines, the first one being an approach where genetically altered viruses, sometimes including transcripts that induce production of cytokines to improve *in situ* inflammatory response, target cancerous cells, infecting and replicating inside them, activating the immune system against specific tumour antigens (Delgado-López et al., 2020; Ma et al., 2021). Regarding GB there is data supporting efficacy and safety of this technique with GB stem cells, Herpes simplex and Zika virus being the most used, the latter for its tendency to infect neural precursors cells; but additional studies are still needed for this to become a more standard therapy option (Ma et al., 2021; Xu et al., 2020). Vaccination against tumours, particularly a GB vaccine targeting EGFRvIII

mutation underwent clinical trials demonstrating safety and efficacy but failed in significantly reducing OvS (Ma et al., 2021). Dendritic cells loaded with cancerous cells or lysates form another type of peptide vaccines explored for cancer treatment which have shown some success in GB (Ma et al., 2021; Xu et al., 2020). Cytokine therapy using interleukins and interferons has been approved for cancers like renal carcinoma or melanoma and has potential to be used in glioma, however further studies and clinical trials are needed to establish stronger scientific evidence regarding this possible treatment (Xu et al., 2020). Tumour-associated macrophages (TAM) therapy relies on antagonizing TAMs since they promote tumour progression, cell migration and, specifically in glioma, angiogenesis. This technique has potential but has only yet been tested in *in vivo* models and modest clinical trials (Xu et al., 2020). Lastly, chimeric antigen receptor T (CAR-T) cells have been developed and tested on mouse models for glioma treatment targeting EGFRvIII, HER2 and other antigens revealing promising tolerance results and even a case of complete remission. By targeting cancerous cells with precision, this therapy increases efficacy while simultaneously reducing toxicity. Various clinical trials are currently in progress (Xu et al., 2020).

Combining multiple immunotherapies might be the way to go moving forward as it should prevent the emergence of resistant subtypes of cancer cells, although it could lead to exacerbated side effects and difficulty to determine which of the treatments is displaying actual results (Delgado-López et al., 2020; Ma et al., 2021; Xu et al., 2020).

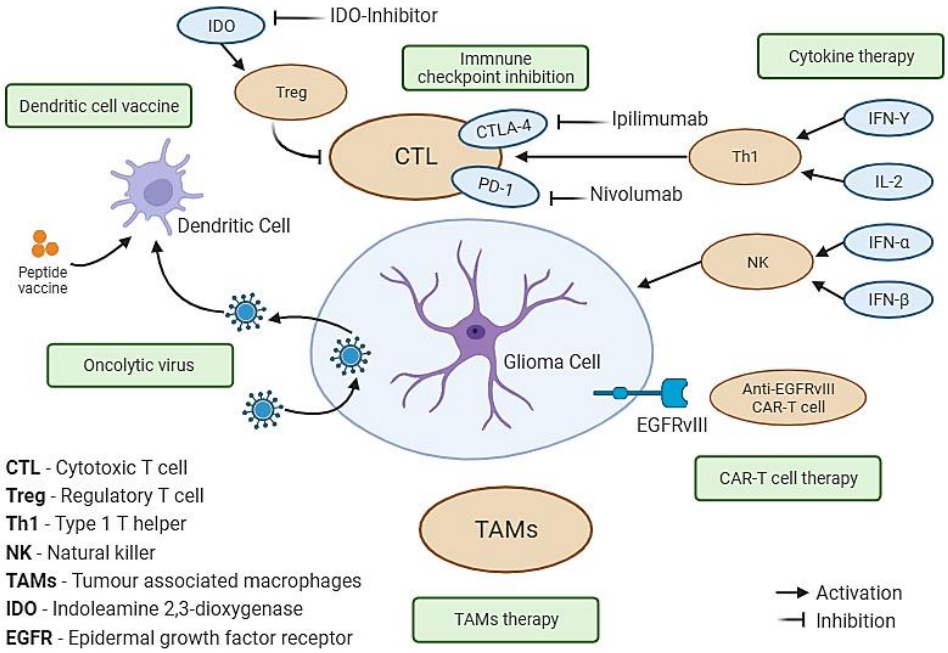

Figure 6 *- Representation of the mechanism of action of some potential new immunotherapy treatment options for glioma treatment. Adapted from* (Xu et al., 2020) *using BioRender*.

Osteosarcoma

Overview, prognostic, and challenges

Osteosarcoma (OS) belongs to the group of bone and joint cancers, where majority of new cases appear before the age of 20 years old (24.2 %), as seen in figure 7a. Nevertheless, the median age at diagnosis is 46 and the median age of death falls in the age group of 65 to 74, at 66 years old, as shown in figure 7b (National Cancer Institute, 2023). Although OS is very rare, with only about 400 cases per year, it is the number one primary bone and joint cancer, as more than half of all bone sarcomas are OS (C. Chen et al., 2021; Gill & Gorlick, 2021). Most located in long bones as well as spine and pelvis, it has a high capacity to invade other tissues, leading to early metastasis, particularly in the lung, where mortality is elevated (Gill & Gorlick, 2021; Nirala et al., 2023). These tumours are classified as either osteoblastic, chondroblastic or fibroblastic based on their histological pattern, even though this cancer is very heterogenous and therefore hard to sub-classify due to most tumours having multiple patterns (Gill & Gorlick, 2021). There are two main peaks in incidence: one in teenage years, due to the growth peak that happens around this time, and one after the 65-age mark, mostly because of Paget disease (Gill & Gorlick, 2021). The survivance rate over 5 years of around 68 % in cases of localized tumour (which amounts to 85 % of OS) treated with standard care, consisting of surgery and CT, drops to 20 to 30 % in case of metastatic disease or recurrency (C. Chen et al., 2021; Gill & Gorlick, 2021). This cancer has a high recurrency frequency due to resistance to CT drugs mostly related to CSCs (C. Chen et al., 2021). No progress has been made over the last three decades regarding the prognosis of this disease, although classifying OS into different subgroups based on their genomic alterations, makes approaching a future precision medicine treatment easier (C. Chen et al., 2021; Gill & Gorlick, 2021; Nirala et al., 2023).

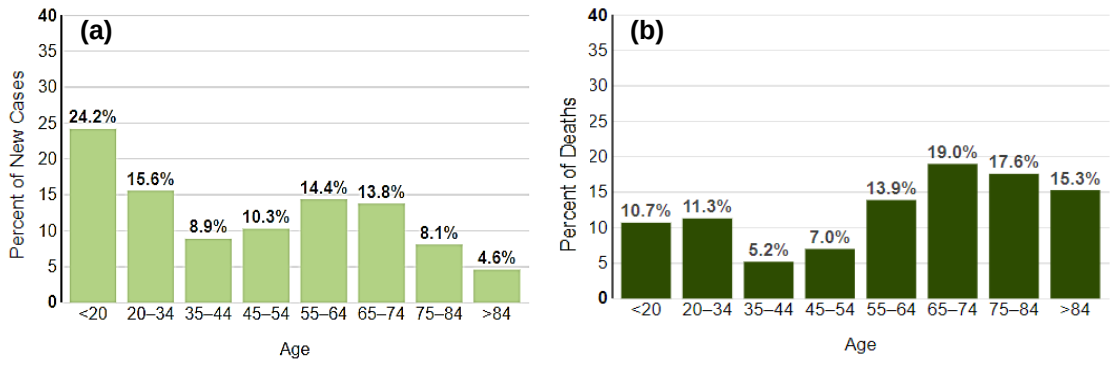

Figure 7 *– (a) Percentage of new cases of bone and joint cancer by age group from 2016 to 2020 and (b) percentage of deaths by bone and joint cancer in the same period* (National Cancer Institute, 2023).

Mechanisms of carcinogenesis

As in most cancers, tumorigenesis is complex and happens due to a combination of different reasons and processes. OS emerges from the mesenchymal cells that form the bone and is associated with major genetic instability, chromosomal abnormalities, and rearrangements; for instance, the presence of chromothripsis in about 77 % of OS cases, which is related to tumour progression and, therefore, a worst prognosis (Harada et al., 2015; Nirala et al., 2023). This event is described as a mutation where multiple chromosomal relocation occurs at once in a small genomic region and is stated to contribute to amplification of oncogenes and inactivation of tumour suppressor genes, two other processes deeply related to carcinogenesis (Cortamp et al., 2020; Swift & Golsteyn, 2016). Multiple tumour suppressor genes are commonly inactivated in OS, namely *rb1*, *atrx* and *dlg2*, but *tp53* is the most common, with the p53 pathway found altered to some extent in all OS cases (Gill & Gorlick, 2021; Nirala et al., 2023). Other genes related to OS carcinogenesis are tumour promoting genes *myc* and *mdm2* which are usually hyperactive in this cancer; MYC takes part in regulation of cell cycle in addition to other relevant events regarding cell viability and metabolism, and MDM2 inhibits p53 (Nirala et al., 2023). Besides this, epigenetic alterations also have a crucial role in the pathogenesis of many cancers, that being the case of OS. The immune system, as expected, has an impact in tumorigenesis of OS by regulating tumour development and proliferation. This occurs through dysregulation of signalling pathways such as PI3K/AKT/mTOR, JAK/STAT, RTKs and others, influencing metastasizing and resistance to chemotherapy (Nirala et al., 2023).

Current treatment and therapeutic approaches

There are very few molecules known to be effective in treating this disease, meaning the standard treatment for localized OS consists of CT using three different drugs out of the five that are active on this type of tumour: methotrexate, doxorubicin, cisplatin (the most common trio), ifosfamide and etoposide; administered before and after surgical resection (Gill & Gorlick, 2021; Nirala et al., 2023). In metastatic and relapsing cases, surgery to remove metastasis is the main treatment option as well as CT with ifosfamide and etoposide or gemcitabine and docetaxel (Gill & Gorlick, 2021). Although the combination of surgery and CT to treat OS cases has proven to improve results, it is still insufficient on more aggressive tumours, hence the introduction of immunotherapy as a new way of treating these patients (C. Chen et al., 2021).

Innovation and potential new treatment options

Subcategories of OS have been differentiated through better understanding of its biological properties and molecular characterization. Thus, allowing the development of innovating approaches through personalized medicine, mostly immunotherapies (C. Chen et al., 2021; Gill & Gorlick, 2021). Proteins such as B7-H3, GD2 and HER2 are present at OS cells surface allowing the use of antibody-drug conjugates as a possible therapeutic approach (Gill & Gorlick, 2021). Other options include onco-vaccines, cytokines, genetic altered T cells or a combination of these (C. Chen et al., 2021). Cancer vaccines boost the immune system reaction to tumours by developing antibodies specifically against antigens that exist at the cancer cell surface (C. Chen et al., 2021). Vaccines based on dendritic cells are the most common but although immune response is improved, success in OS is limited (C. Chen et al., 2021). Some cytokines can boost proliferation and differentiation of T and B cells and induce Natural Killer (NK) cells but for dosages to be efficient, toxicity occurs in patients of OS (C. Chen et al., 2021). CAR-T cells showed great potential for treating HER-2 positive sarcomas, even when HER-2 expression is low, which is the case in OS, without toxicity that required restricting dosage (C. Chen et al., 2021). Although all these different immunotherapies are available and currently under clinical trials, most results fall short of expectations regarding efficacy in solid tumours such as OS, making treatment possibilities for this cancer still very limited (C. Chen et al., 2021; Nirala et al., 2023). To contradict this tendency, it is necessary to identify more adequate immune checkpoints and decrease toxicity of current immunotherapy (C. Chen et al., 2021).

OS cells express several RTKs which led to the use of tyrosine kinase inhibitors (TKIs) as treatment in relapsed and non-reactive cases (Gill & Gorlick, 2021). Some of these drugs are Sorafenib, Regorafenib, Cabozantinib, Lenvatinib and Pazopanib. Combining TKIs with already used chemotherapeutic agents such as Lenvatinib and Etoposide or Sorafenib and Everolimus was considered but overlapping toxicities and lack of better results interrupted treatment (Gill & Gorlick, 2021). The possibility of using TKIs as maintenance treatment after CT is under evaluation but prospects are set on finding active new drugs targeting other signalling pathways implicated in OS tumorigenesis, who are active on their own in relapsed cases, with different toxicities to the ones already used so that combining them is easier and there is lesser need to adapt dosages of the currently used CT (Gill & Gorlick, 2021; Nirala et al., 2023). Numerous drugs are in the clinical trial process indicating good results, but there is always the possibility of developing resistance as cancerous cells are usually able to compensate targeted therapies by acquiring replacement paths to their end goal (Nirala et al., 2023).

TMBIM4 and its importance on hallmarks of cancer

The Transmembrane BAX Inhibitor-1 Motif-containing (TMBIM) family is a group of six cell death regulatory proteins, TMBIM1 to TMBIM6, capable of altering cellular adhesion, metabolism, motility, and calcium (Ca^{2+}) fluxes (Almeida et al., 2020; Carrara et al., 2017; Rojas-Rivera & Hetz, 2015). TMBIMs are cation channels located at different intracellular organelle membranes (Figure 8). TMBIM4, also known as human Golgi anti-apoptotic protein (hGAAP), is an ion channel (figure 8) located in the membrane of the Golgi complex. It has a fundamental importance for cell viability, as it regulates Ca^{2+} intracellular fluxes from the Golgi and the response of the cell to apoptotic stimuli. Thus, the increase of TMBIM4 expression leads to a higher resistance to apoptotic stress (Almeida et al., 2020; Carrara et al., 2017). Ca^{2+} influx can occur via store operated Ca^{2+} entry (SOCE) in response to reduced Golgi Ca^{2+} concentration due to TMBIM4 overexpression. The consequent activation of SOCE by TMBIM4 has been linked to increased cell motility by contributing to focal adhesion turnover through activation of a Ca^{2+}-dependent protease named calpain2 (Saraiva et al., 2013). Studies from our group showed that cell invasion through extracellular matrix was also stimulated by tumour cells overexpressing TMBIM4, thus advocating that this protein has a crucial impact in the metastatic process, projecting the tumour from early to invasive stages. For instance, it was found that TMBIM4 overexpressing cells enter the lungs and are more easily retained there than control cells. Additionally, TMBIM4 silenced cells had much lower invasion rates versus control cells (Almeida et al., 2020). TMBIM4 overexpression leads to an increase in adenosine triphosphate (ATP) production and oxygen (O_2) consumption, by increasing mitochondrial respiration. Therefore, leading to an accumulation of reactive oxygen species (ROS), impacting cell migration and invasion. ROS levels are higher in cells overexpressing TMBIM4 and that is known to have a part in cell motility and adhesion, particularly H_2O_2, that is a relevant second messenger on which the cell depends for controlling processes such as metabolism and invasiveness (Almeida et al., 2020). Unpublished data from our group suggest a strong correlation between increased TMBIM4 mRNA levels (TCGA data) in gliomas and a reduced survival rate in glioma patients. Thus, suggesting that TMBIM4 is indeed associated with cancer progression and that it could possibly be used or as a cancer biomarker. All these data support that this protein has the potential to be used as a therapeutic target to control various hallmarks of cancer or as a biomarker for cancer progression. The work presented here is focused on glioma and OS, both very invasive types of cancer. Consequently, the impact of TMBIM4 expression dysregulation on these cancer types was studied.

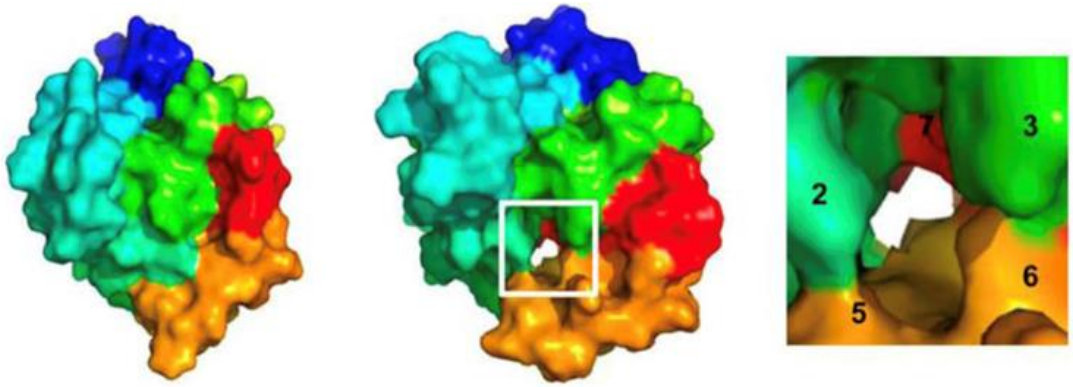

Figure 8 *– TMBIM4 predicted structure, based on the bacterial homologue, adapted from* (Carrara et al., 2017). *The ion channel pore is highlighted by a white square and the numbers represent the transmembrane domains.*

Objective

The main goal of this work was to evaluate the impact of TMBIM4 in tumour progression-related cellular processes, such as cancer cell survival and proliferation, and therefore explore the potential mechanisms underlying the observed correlation between TMBIM4 expression and patient prognosis and survival, particularly in OS and glioma tumours. As explained above, this protein influences many different processes regarding cellular motility and metabolism and consequently tumour progression and metastasis. This way, we hypothesise that TMBIM4 may be a good biomarker for these cancers and may eventually be useful in the clinical context.

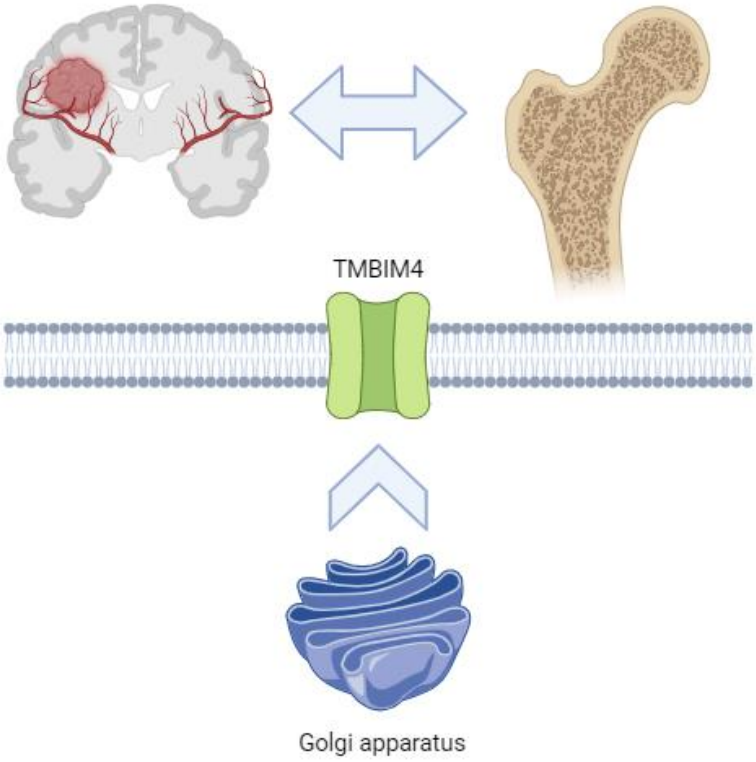

Figure 9 *– Schematic illustration representing the impending impact of TMBIM4 in glioma and OS. Created using BioRender.*

Chapter II – Role of TMBIM4 on glioma cell viability and proliferation

Methods

Cell culture

The cell lines used in this work are primary human GB. The U87 line was provided by Dr Diogo Castro from the *Instituto Gulbenkian da Ciência* (IGC) and *Instituto de Investigação e Inovação em Saúde* (i3S) while the U251 GFP line was provided by Dr Hélène Castel from Normandie University. Cells were maintained in T-25 and T-75 flasks (VWR) with Dulbecco's Modified Eagle's Low Glucose Medium (DMEM, Corning) complemented with 10 % Fetal Bovine Serum (FBS, Corning) and 1 % Penicillin-Streptomycin Antibiotic (PEN-STREP, Grisp). U87 cells were supplemented with 1 % Non-Essential Amino Acids (MEM NEAA 100x, Gibco®) and U251 with Puromycin Antibiotic (4 µg/mL, Alfa Aesar) for GFP gene maintenance. Both were kept in an incubator (Esco CelCulture®) with 5 % CO_2 at a temperature of 37 º C.

Sub-cultivation was performed in the vertical laminar flow chamber (Esco Class II Biological Safety Cabinet (BSC)) when cells were at 80 % confluence. After removal of the medium and the addition and subsequent disposal of Phosphate Buffer Saline (PBS, Corning) for washing, trypsin (Sigma) was added to detach the cells from the flask surface for 2 to 3 minutes in the incubator. After detaching the cells, trypsin action was inactivated by adding medium to that same flask. Finally, the detached cells were homogenized by resuspension and transferred to a new flask. To know the necessary number of cells for seed for each assay, the density of cells in the suspension was verified using the formula presented in figure 10, which provides the existing number of cells/mL of suspension.

$$\text{Cell density (cells/mL)} = \frac{\sum Cells\ per\ quadrant}{number\ of\ quadrants\ counted} \times 10^4$$

Figure 10 *– Equation for determination of cellular density.*

For the cell counting procedure the Neubauer Chamber, that consists of grids divided into 4 quadrants (figure 11b), was used as seen in figure 11a. The grid area was first covered with a coverslip, and then 10-12 µL of cell suspension was pipetted into one of the two chamber compartments. The chamber was placed on the inverted microscope (Olympus CKX41) for observation. Counting was done quadrant by quadrant, in zigzag, as represented in figure 11c, discarding cells under two consecutive sides chosen by the operator (figure 11d). After counting, the average between the values obtained in each quadrant was calculated.

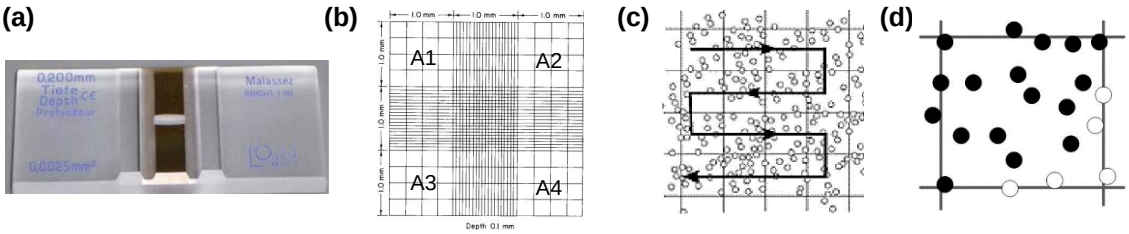

Figure 11 *– Cell counting procedure using the Neubauer Chamber (also known as Hemacytometer). (a) Neubauer chamber* (Santos & Mariano, 2014). *(b) Chamber dimensions and an indication of the four lateral quadrants (A1 to A4) and the central quadrants adapted from* (Absher, 1973). *(c) Counting method in zigzag* (Santos & Mariano, 2014). *(d) Example of two laterals discarded in the counting process* (Barbedo, 2013).

3D cell culture

Cell spheroid production was initiated by depositing U87 cells, previously transfected with siRNA on the inside of the lid of 35 mm Petri dishes (VWR). Every plate contained 4 drops, each with 50 µL of cell culture, corresponding to 5 x 10^4 cells. After applying the drops to the lid, the plate was closed with a quick up and down movement to prevent the drops from losing their shape by sliding out of place. Spheroids formed after 24-48h in the incubator. 5 mL of PBS was added to each Petri dish to prevent the cell-containing drops to lose volume during the spheroid formation period.

siRNA transfection

This procedure required cells to be at 60 to 70 % confluence at the moment of the transfection. Thus, 1.0 x 10^5 cells were seeded in a 12-well plate well (VWR) the day before transfection. The following day 45.9 µL of OptiMEM (Gibco) and 2.25 µL of siRNA (100 nM) were added to tube 1 while tube 2 contained 43.2 µL of OptiMEM and 4.8 µL of oligofectamine transfection reagent (invitrogen). After incubation at room temperature for 5 to 10 min, tube 2 was added to tube 1, forming the vesicle with siRNA to be transfected. After incubating again for 20 min at room temperature, 30 µL of this mix was

added dropwise to each well. The transfected siRNA contained a sequence that silenced TMBIM4, which can be seen below in table 2.

***Table 2** – Double-stranded oligonucleotide sequence used in TMBIM4 transfection*

siRNA	Sequence sense and antisense	Gene KD	Source/Reference
TMBIM4 siRNA #1	Sense 5'-CGAUCGAGGACGACUUCAACU-3' Antisense 5'- UUGAAGUCGUCCUCGAUCGAG-3'	TMBIM4	(Gubser, Bergamaschi, Hollinshead, Lu, Kuppeveld, et al., 2007)
TMBIM4 siRNA #2	Sense 5'-CUGUACGGACAUUUGUACAUG-3' Antisense 5'- UGUACAAAUGUCCGUACAGAC-3'	TMBIM4	
Control siRNA	Proprietary sequence from Invitrogen	GFP	Invitrogen

pcDNA transfection

Plasmid DNA (pcDNA) transfection was performed with 1.0 x 10^5 cells seeded the day before in 300 µL of antibiotic-free DMEM in a 48-well plate well (VWR) so that cell confluence was 70 % at the moment of transfection. In this case, the plasmid ptdTomato-C1 (clontech) encodes the tandem dimer Tomato (tdTomato) gene, a red fluorescent protein. After the procedure, cell lines should express free tdTomato. In the case of the U251 cells, they also express the green fluorescent protein (GFP). The transfection reagent used was XtremeGene9 (Roche). The protocol started by preparing tube A which contained 5.5 µL of OptiMEM (Gibco®) and 2.0 µL of the reagent, and tube B contained 6.75 µL of OptiMEM and 0.75 µL of plasmid (at 200 µg/mL), each tube containing a total of 7.5 µL. Tube A+B was incubated for 15 min at room temperature, followed by pipetting 15 µL into each well to be transfected. Image acquisition was performed on a Zeiss Axiobserver microscope using an x20 objective and ZEN software.

Kill curve with geneticin

To select the cells that present the previously transfected pcDNA, geneticin was used, since the plasmid had a resistance gene to this antibiotic. For this, a cell death curve was performed with a stock concentration of geneticin 50 mg/mL (Gibco®), to obtain the minimum concentration required to induce the death of the non-transfected

cells. Several concentrations were tested, choosing for selection the lowest concentration that led to the death of all cells in the well after 6 days. After seeding U87 and U251 cells in 48-well plates (4 x 10^4 U87 cells and 6 x 10^4 U251 cells), and when their confluence was 30 %, geneticin was added at concentrations of 0 (control); 0.5; 1; 1.5 and 2.0 µg/mL for both lines. A medium exchange was performed every two days.

MTT cellular viability assay

The MTT (3-(4,5-dimethylthiazol-2-yl)-2,5-diphenyltetrazolium bromide, Sigma) cell viability assay measures the ability of mitochondria to reduce MTT reagent to formazan crystals, according to figure 12a. These crystals are only formed if mitochondria are metabolically viable. This assay was used to analyse the impact of reducing TMBIM4 expression and to assess the resistance of U251 and U87 cells to TMZ. The first procedure started 24 hours (h) after transfecting cells with siRNA by seeding 1.7 x 10^4 previously transfected cells in each well of a 96-well plate with 200 µL of DMEM. After 48 h (total of 72 h post transfection), a wash was performed with warm PBS, and MTT was added to each well. This reagent was prepared previously by dissolving 0.5 mg/mL in a heated culture medium, added to the cells, and incubated for 2 h at 37 °C. After washing with warm PBS, 200 µL of dimethyl sulfoxide (DMSO, EMSURE® ACS) was added to every well. This reagent solubilizes the crystals that formed and precipitated at the bottom of the wells. The scale of purple coloration is shown in Figure 12b. The absorbance is measured at 595 nm in a Multiskan FC reader (Thermo Scientific™, USA). This methodology was also applied to determine the concentration of TMZ with the greatest impact on the viability of both cell lines. The procedure was identical except that the cells used are non-transfected and the cell viability measurements were performed at 24, 48 h or 72 h, instead of 72 h in the case of the first assay.

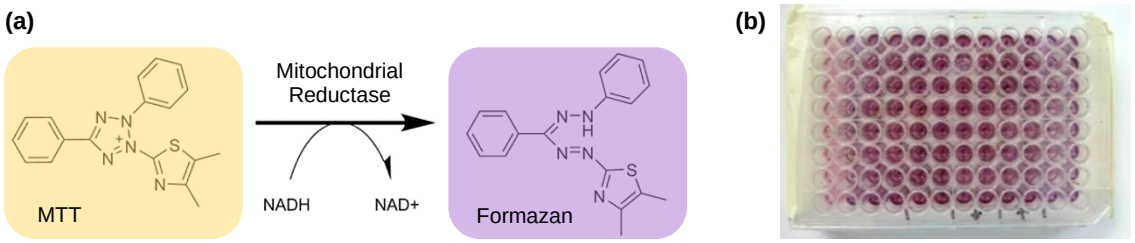

Figure 12 *– (a) Equation that represents the MTT reduction to formazan by mitochondrial reductase, indicating the colour of the reagent and product adapted from* (Präbst et al., 2017) *(b) Example of plate obtained after MTT assay* (Sularsih et al., 2019).

Cellular proliferation assay

Variations in cell biomass were estimated at 24 h, 48 h, 4, 5, and 6 days, using the crystal violet proliferation assay. On the first day of the assay, 1.4 x 10^3 U251 cells and 1.0 x 10^3 U87 cells were seeded in 200 µL of DMEM in 96-well plates. This way, the wells were at a confluence of about 20 % the next day. On day 1, which corresponds to the 24 h test, the medium was removed by washing with 100 µL of 1x PBS before adding 100 µL of 10 % crystal violet solution in 96 % ethanol for 10 minutes. After, the plate was washed with plenty of water, and a solution containing 10% ethanol and 1 % acetic acid was added before the absorbance was read in the Multiskan FC microplate reader at 595 nm. This was repeated at the indicated time points.

Cellular viability assay in 3D culture

Propidium iodide (PI, Sigma), at a final concentration of 0.5 µg/mL, was added to previously performed 3D cell cultures and incubated for 20 min at 37 °C. When a cell is alive, its membrane is impermeable to PI, preventing it from entering the cell. DMSO (10 %) was used as a cell death inducer for this assay, which allows PI to enter the spheroid cells. This method granted analysis of cell viability in 3D and eventually will allow to validate how the transfection affected the spheroid cells viability. Image acquisition was performed with a Zeiss Axiobserver microscope using x20 objective and ZEN software, used to measure the average intensity of the PI fluorescence emitted by the area of the spheroids.

Statistical analysis

Statistical analysis was performed in GraphPad Prism software version 8.0. Error bars indicate the standard deviation (SD) or standard error of the mean (SEM) as indicated in the figure legends. Data was analysed using the T-student test, Logrank, or one-way ANOVA analysis with Turkey or Kruskal-Wallis's test and Dunn post-test. Significant results are highlighted with * $p<0.05$, ** $p<0.01$ or *** $p<0.001$.

Results and Discussion

Assessment of TMBIM4 impact on proliferation and viability of U251 and U87 cells

The results presented below in figure 13 show that cell viability was not significantly affected on both U251 and U87 cell lines by the reduction in TMBIM4 expression following siRNA transfection. This result is visible at 72 h post-transfection since the percentage of viable U251 and U87 cells transfected with siRNA1 and siRNA2 were kept above 90 % and close to control values. This data is complemented by the crystal violet assay results in figure 14 since it shows that siRNA transfection does not affect cellular proliferation. This information allowed for the development of protocols to assess the impact of TMZ on 3D cell culture.

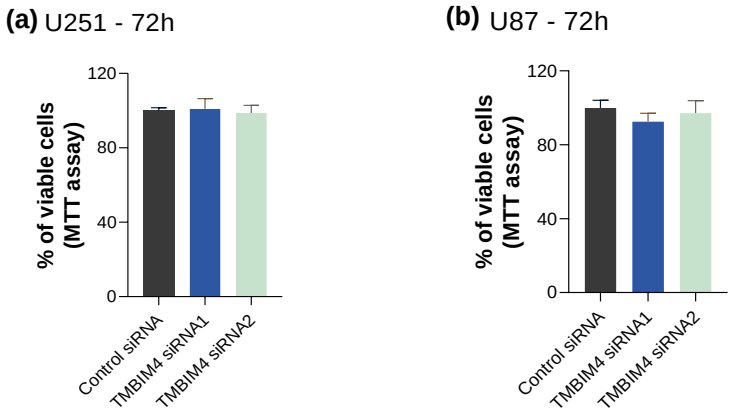

Figure 13 *– MTT viability assay results in U251 (a) and U87 (b) cell lines. Percentage of U251 (a) and U87 cells (b) transfected with control siRNA, siRNA1, and siRNA2 viable at 72h after the beginning of the assay. Results are shown as mean ± SD from a representative experiment from 3 independent experiments, Student's t-test compared to cells transfected with siRNA. Differences between results were not significant.*

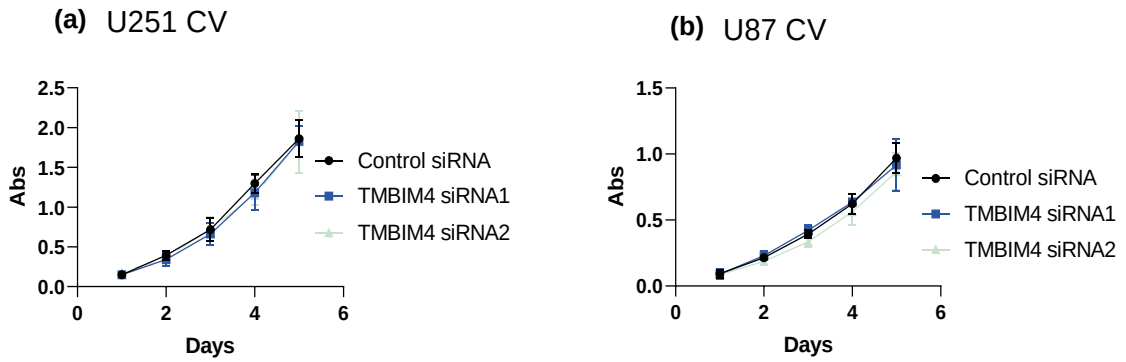

Figure 14 *– The crystal violet absorbance of the three conditions (siRNA control, siRNA1 e siRNA2) was measured on days 1, 2, 4, 5, and 6 of the crystal violet viability essay with U251 (a) and U87 (b) cells. Results are shown as mean ± SD from a representative experiment from 3 independent experiments, Student's t-test compared to cells transfected with siRNA in each time point. Differences between results were not significant.*

Preliminary evaluation of TMBIM4 influence on 3D viability of U87 cells

To test U87 cell viability in 3D culture a protocol with PI was applied. If the cell is viable this reagent is unable to cross its cellular membrane; on the contrary, if cell death is present, PI crosses the membrane staining the cell nucleus red. In figure 15, treatment with 10% DMSO was used on U87 as a positive control for cell death. DMSO toxicity killed the U87 cells, meaning that the red seen in figure 15 (d-f) represents non-viable spheroids, validating this assay for the evaluation of U87 cells viability in 3D cell culture. Through a collaboration with i3S, an assay to assess the viability of U87 and U251 cell lines when under silencing of TMBIM4 is being developed.

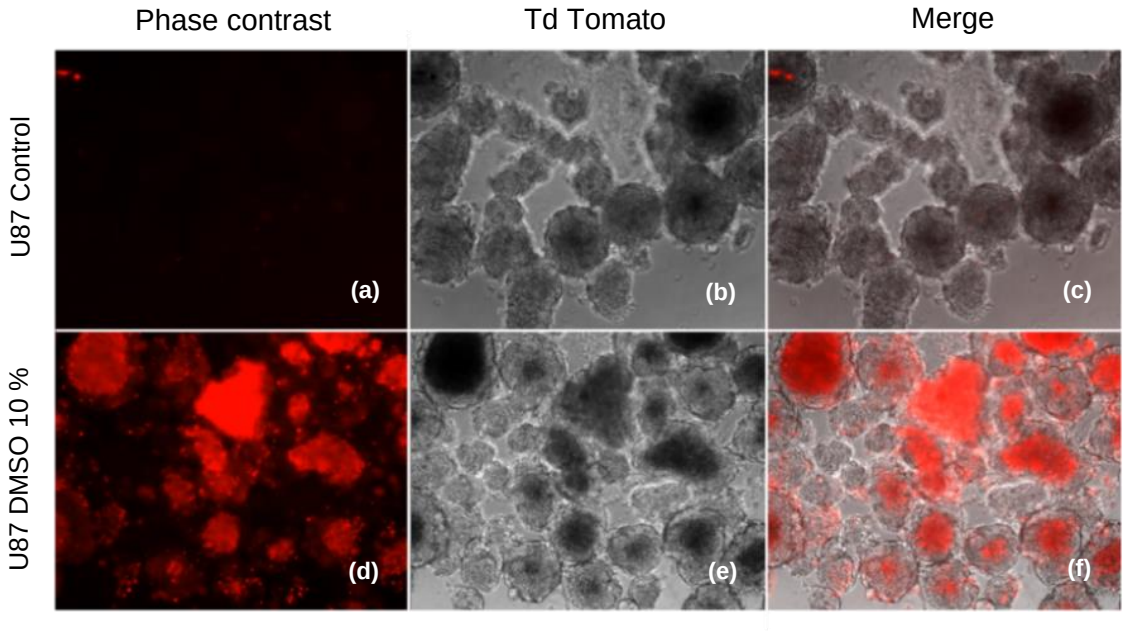

Figure 15 *– Spheroids at the fluorescence microscope treated with PI. The U87 control (a-b) shows U87 cell line without DMSO, while U87 DMSO 10 % (d-f) shows the positive control, with DMSO. Red colouring represents PI-positive non-viable cells.*

Impact of TMBIM4 knock-down on TMZ resistance

Considering the importance of TMZ in the treatment of GB, the impact of TMBIM4 lower expression on the effect of TMZ was assessed. This protocol was developed to assess the effect of TMBIM4 expression reduction on U87 and U251 cell resistance to TMZ. The TMZ concentration optimization on both cell lines was done through MTT viability assay to determine the half-maximal inhibitory concentration (IC50), that is, the minimum concentration necessary to cause death to 50 % of cells. In these assays, DMSO was used as a solvent, since TMZ is solubilized in DMSO. However, DMSO is cytotoxic at the concentration used as control, since the

concentration used corresponded to the highest concentration of TMZ being tested, and the same in every TMZ concentration level. Because of this, the results were inconclusive since it was impossible to determine if cell death occurred due to TMZ or DMSO. Figure 16 presents data from these first assays where DMSO concentration cloaked the results since cells most likely died from DMSO excess instead of TMZ. It is relevant to note that the TMZ ranges used in literature for these cell lines vary greatly, which enforced the necessity to test many different concentrations, as seen below.

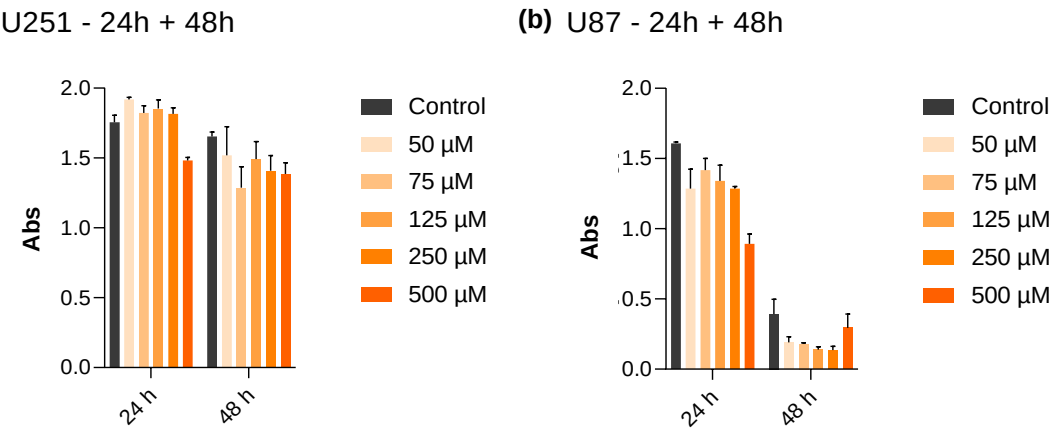

Figure 16 *– First MTT viability assay at 24 and 48h in U251 (a) and U87 (b) cell lines treated with TMZ concentrations varying from 0 and 500 µM to assess cell resistance to TMZ. Preliminary data. No statistical analysis was performed since it was an optimization step.*

After some experimental adjustments, namely carrying out a DMSO control for each concentration of TMZ used and determining the correct TMZ concentration and incubation time to evaluate MTT results, the assay was optimized and repeated. The data obtained are data shown below in figure 17. Data for U87 cells seen in figure 17b indicates that the percentage of viable cells under treatment with 125 µM TMZ is lower when TMBIM4 is silenced, compared to cells transfected with the control siRNA. The same cannot be said about U87 cells under 250 µM TMZ concentration. Regarding the U251 cell line in both 75 µM and 125 µM concentrations, the reduction in viable cells was not significant when compared with cells transfected with the control siRNA (figure 17a).

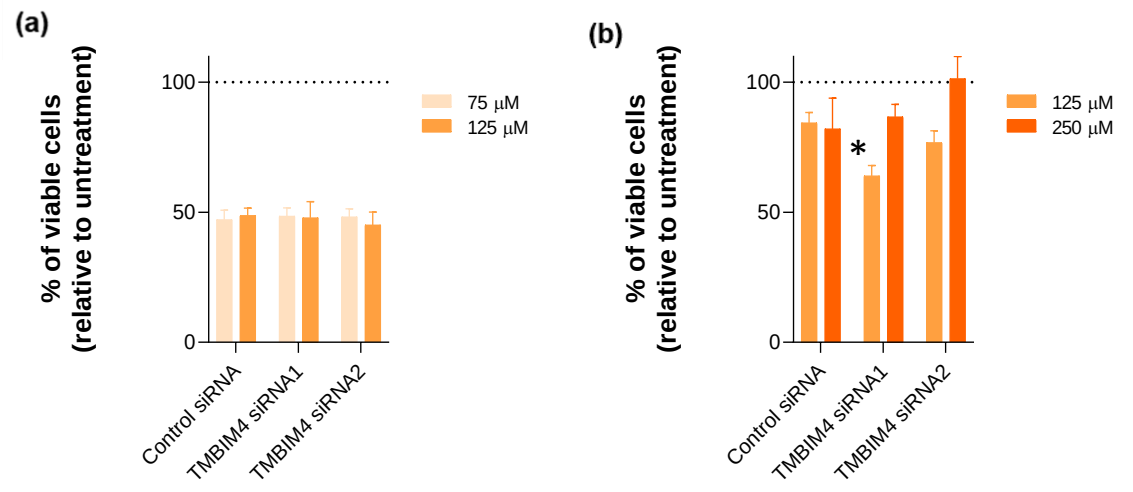

Figure 17 *– Percentage of siRNA-transfected U251 (a) and U87 (b) viable cells after treatment with TMZ concentrations varying from 75 and 250 μM. Incubation time was 72 hours. Results are shown as mean ± SD from a representative experiment from 1 independent experiment, *p<0.05 (Student's t-test compared to control siRNA cells treated with the same concentration of TMZ).*

Impact of TMBIM4 overexpression in U87 and U251 proliferation

The generation of BG cell lines overexpressing TMBIM4 is essential to evaluate the effect of the observed increased expression of TMBIM in GBs. Tho generate GB cell lines overexpressing TMBIM4, a plasmid coding for a fusion protein of TMBIM4 with tandem Tomato (tdTomato) were used. This plasmid contained an antibiotic (geneticin) resistance gene to select for transfected cells. To determine the optimum geneticin concentration to select transfected cells, a kill curve with geneticin was performed for both cell lines. Figure 18 shows the results, where the U87 cell line was tested for 0.5 and 1.0 mg/mL and U251 cells for 1.5 and 2.0 mg/mL. Geneticin concentrations that kill all cells after one week were selected. These corresponded to 1.0 mg/mL and 2.0 mg/mL, to U87 and U251 respectively, and were added to cells every 48 hours after the transfection procedure.

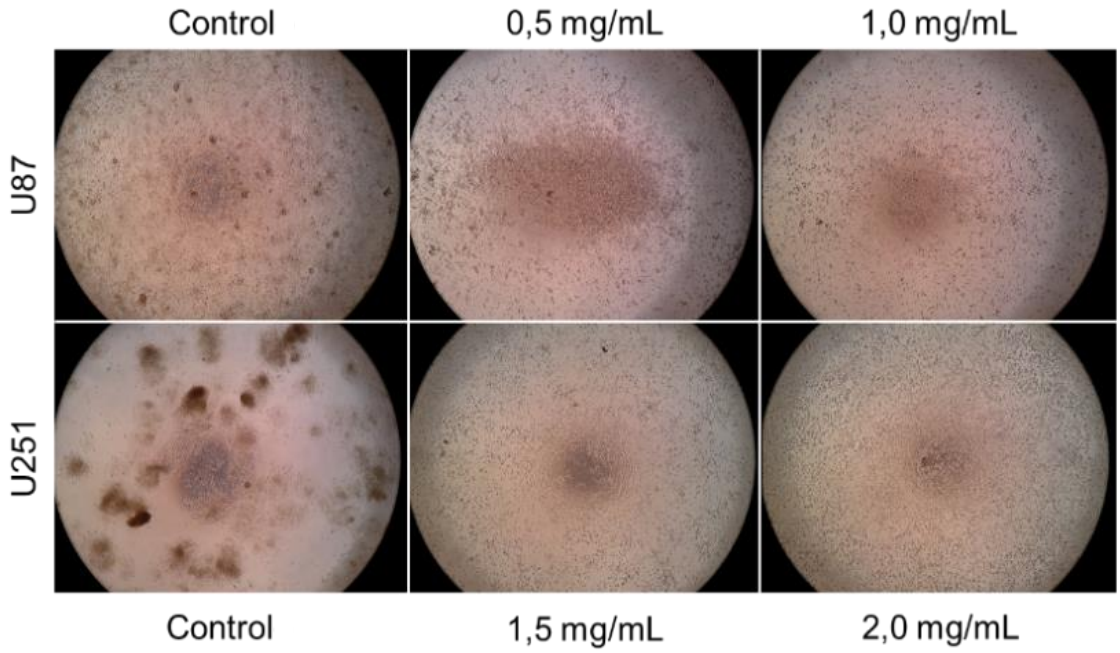

Figure 18 *– Kill curve of geneticin in U87 cells (upper row) in concentrations of 0.5 and 1.0 mg/mL, and in U251 cells (bottom row) in concentrations of 1.5 and 2.0 mg/mL.*

To assess the efficacy of the transfection and selection protocol in these cell lines, the U87 and the U251-GFP cell lines were transfected with the TdTomato plasmid (without TMBIM4) and selected for several weeks with antibiotic. Figure 19 shows the results obtained after transfection with TdTomato on both cell lines. Results from U87 cells (upper row) were non-satisfactory most likely because this cell line is very genetically unstable, meaning that every small disturbance can lead to failed results. These cells also lost TdTomato expression overtime. U251-GFP successfully expressed TdTomato and GFP genes as can be seen on the bottom row of figure 19.

After optimizing the transfection, the plasmid encoding the TdTomato and the TMBIM4-TdTomato fusion was transfected on U251 cells. Results obtained are presented below in figure 20. U251 TdTomato expression (upper row) acts as control since it is the model plasmid and was used to optimize the method. In figure 20 bottom row we can see TMBIM4 in red, and consequently the Golgi complex since this is a Golgi protein, due to the transfection with the plasmid. These cells were maintained in culture with geneticin selection of 0.5 mg/mL. Further characterization of the obtained cell lines will be performed. Namely, the co-stain with another Golgi-resident protein to confirm the TMBIM4 subcellular localisation.

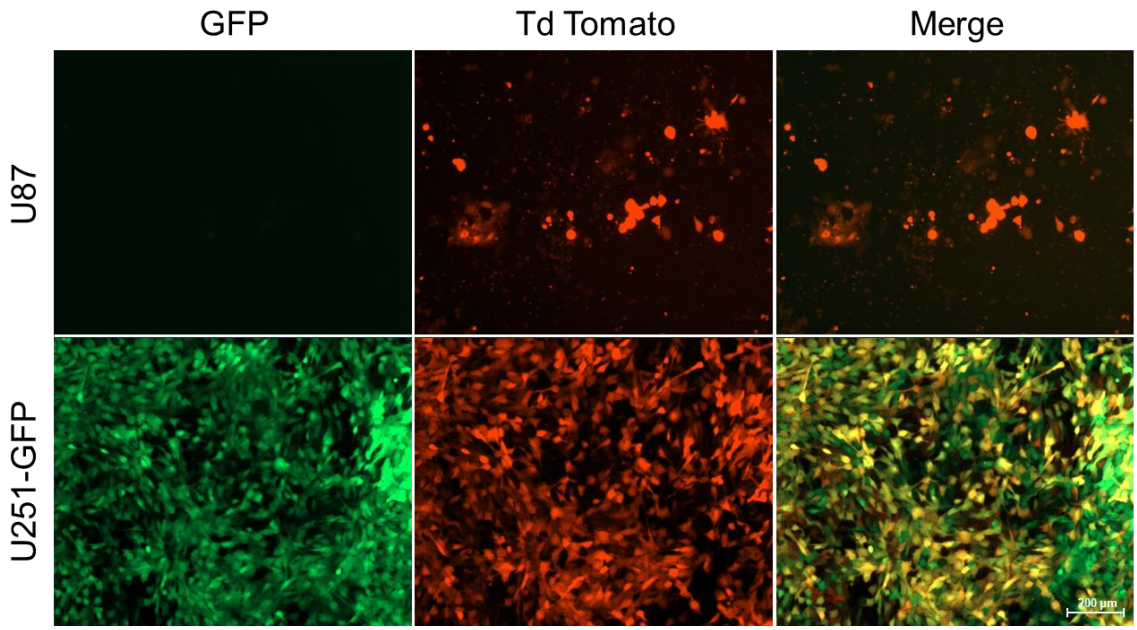

Figure 19 *– U87 cells (upper row) and U251-GFP (bottom row) transfected with TdTomato (in red) observed at the fluorescence microscope. Preliminary assay. Scale bar of 200 µm.*

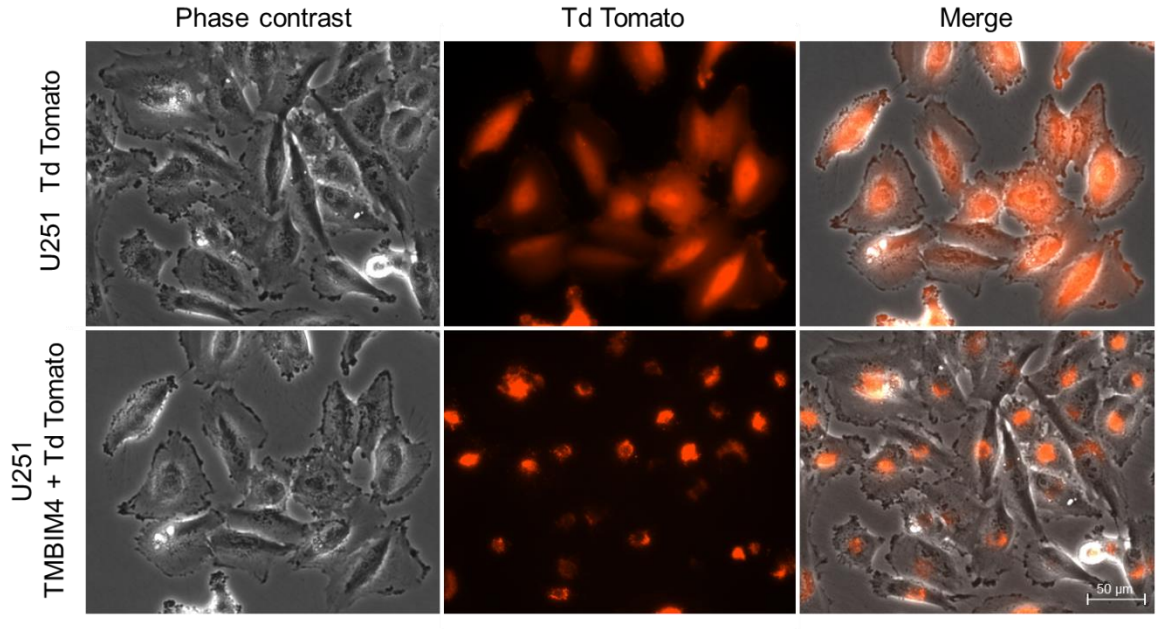

Figure 20 *– U251 cells transfected with TdTomato (upper row) and U251 transfected with TdTomato-tagged TMBIM4. Image obtained at 40x zoom. Scale bar of 50 µm.*

Chapter III – Role of TMBIM4 on osteosarcoma cell survival

Methods

Cell culture in normal and starvation conditions

The U2OS cell lines were provided by Professor Geoffrey Smith (Oxford University) (Gubser, Bergamaschi, Hollinshead, Lu, Van Kuppeveld, et al., 2007) maintained in T-25 and T-75 flasks (VWR) with DMEM (Corning) complemented with 10 % FBS (Corning) and 1 % PEN-STREP (Grisp). Cells were preserved in an incubator (Esco CelCulture®) with 5 % CO_2 at 37 º C and supplemented with 0.5 mg/mL geneticin antibiotic (Alfa Aesar) every one to two weeks for cell maintenance ensuring that the integrated plasmid is preserved.

To study the impact of TMBIM4 overexpression, the group of Prof Geoffrey Smith developed a model of the protein overexpression pattern as seen in table 3, where Neo cell line corresponds to the endogenous protein, which means its expression level and activity are both low; TMBIM4 has both parameters high and TMBIM4 CtMut has the same protein overexpression as TMBIM4, but is not functional, making it equal to Neo.

Table 3 *– Cell lines description*

	Expression level	**Activity**	
Neo	Low (endogenous)	Low (endogenous)	Emply plasmid pcDNA 3.1
TMBIM4 overexpression	High	High	TMBIM4 overexpression
TMBIM4 CtMut overexpression (Mut)	High	Low (endogenous)	C-terminal Mutant TMBIM4 (not functional) overexpression

Cells were kept at 100% confluence in complete media for 14 days without media changes to more closely mimic the nutrient starvation conditions found in the tumour environment, that is, low accessibility to nutrients and the presence of pro-proliferative signals. Sub-cultivation and cell counting was executed as described for U87 and U251 cell lines in Chapter II ‘Cell Culture’.

Cell treatment

For this assay, cells were kept in starvation conditions as described before. This protocol took place over a period of 14 days. On day one, 2 x 10^4 cells of Neo and Z cell lines were seeded in two 24-well plates, as well as 3 x 10^4 Mut cells. Days 2 to 13 were treatment days, in which cells were treated with H_2O_2 every day and with Catalase (CAT) and Disulfiram (DF) every two days. Photos were acquired with a Zeiss Axiobserver microscope using x20 objective and ZEN software approximately every four days. On day 14, cells were stained with Hoechst in a 5.0 x 10^{-3} concentration.

The solutions used in this assay were prepared beforehand. The initial H_2O_2 stock solution at 9.8 M concentration was kept at 4 °C and used to make the procedure's stock and working solutions. Our stock solution at 0.5 M was prepared every 3 days by adding 51 µL of H_2O_2 and 949 µL of double distilled water (ddH_2O) to an Eppendorf. The working solution (WS) with a concentration of 2500 µM consists of 5 µL of stock solution added to 995 µL of ddH_2O and was prepared every day that cells needed treatment, that is, from day 2 to day 13 of this assay. To obtain a final concentration of 20 µM, 4 µL was added per 500 µL (contents of one Eppendorf tube); in the same way 2 µL was added per 500 µL to obtain 10 µM of final concentration. In a preventive measure to avoid possible operator errors, the volumes pipetted into the 24 well plates with H_2O_2 concentrations of 0.25 µM and 0.5 µM, were done from 250 µM Eppendorfs instead of the 500 µM used on the rest of the wells as that allowed to not pipet volumes below 1 µL, as can be seen on table 4.

Table 4 *– Volumes of working solution (WS) and concentrations used in each well in both 24 and 6 well plates of the U2OS cell cycle assay*

[H_2O_2]	24 well plate		6 well plate
	[500 µM] WS	[250 µM] WS	
0.25 µM	0.5 µL	1.0 µL	1.0 µL
0.5 µM	1.0 µL	2.0 µL	2.0 µL
1.0 µM	2.0 µL	--------	4.0 µL
2.0 µM	4.0 µL	--------	8.0 µL
5.0 µM	--------	--------	20.0 µL

CAT stock solution of 20 000 U/mL was kept at - 20 °C and used to prepare the WS of concentration 400 U/mL by adding 10 µL in 500 µL of final volume. DF stock solution of 50 mM contained 20 mg of DF in 1240 µL of DMSO and was kept at - 80 °C.

The WS consisted of 1 µL of stock solution plus 999 µL of DMSO. To obtain a final concentration of 0.05 µM, 0.5 µL of WS was added in DMSO per 500 µL.

Cell collection for cell cycle analysis by flow cytometry

In this protocol, the cells used were prepared following the exact same treatment scheme as explained in the previous section with the difference that they were harvested at the end. Only cells seeded in the 6 well plates were applied here. The goal of using the flow cytometry technique is to quantify the percentage of cells in the sub-G1 population, which corresponds to dead cells.

After the initial 14-day period of the assay, cells needed to be prepared for the Flow Cytometry technique for sub-G1 determination by being stained with PI. The whole process is done on ice and begins with harvesting the cells into a 15 mL falcon tube, washing them with 1 to 2 mL of PBS, and collecting the PBS into a falcon tube. The attached cells were then harvested with 1 mL of warm EDTA PBS of concentration 1 to 5 mM, previously incubated for 5 minutes at 37 °C, into the same falcon tube using a 1000 µL pipette tip to help with the detachment. Next, a wash with 1 mL of cold PBS was performed by spinning in the centrifuge at 160 g force for 8 min, followed with resuspension in the 100 µL remaining of cold PBS in the falcon tube after removing the 1 mL used to wash. Fixing and permeabilization of the cells were done by adding 1 mL of 80% ethanol at 4 °C drop by drop while the falcon tube was on the vortex at slow speed. After, falcons were incubated for 2 h at 4 °C. Tubes were spined at 200 g for 8 min and then washed twice with 1 mL of PBS using the centrifuge for 8 min, resuspending cells gently with a pipette every time. At the end, cells were resuspended again in 100 µL PBS and then stained through resuspension in 200 µL of PI staining solution, consisting of 25 µg/mL of PI and 50 µg/mL RNase A. PI was kept in stock at 2 mg/mL and RNase A at 5 mg/mL. After incubating the cells for 20 minutes at 37 °C and adding 300 µL of PBS, the samples were ready for running. The red intensity (excitation: 488 nm and emission: 661/16 nm) of each individual cell was measured by flow cytometry using a FACS Flow Cytometer (BD Biosciences) and data was analysed using the FlowJo_V10 software, following doublet cell discrimination and PI-stained dead cell exclusion. Three independent experiments were performed, each including three internal replicates.

Results and Discussion

The overexpression of TMBIM4 but not of a non-functional C-terminal mutant of TMBIM4 lead to an increased ability of cells to survive for long periods (14 days) in culture with low nutrient concentration. Mass spectrometry proteomic analysis of the U2OS cell lines overexpressing TMBIM4 was previously performed by our group to understand which proteins were deregulated when the expression of TMBIM4 was altered. Proteins with a similar expression pattern in Neo and TMBIM4 CtMut overexpression but different from TMBIM4 overexpression were analysed. This included Cystathionine beta-synthase (CBS) and Cystathionine gamma-lyase (CTH), synthetized by genes *cbs* and *cth* respectively and a series of cellular-redox status-related proteins. These two proteins (CBS and CTH) are related to *de novo* cysteine production (H. F. Zhang et al., 2022; Zhu et al., 2019) within the cell. Since TMBIM4 has been previously described to induce the accumulation of H_2O_2, the intracellular levels of this molecule were manipulated artificially to determine if this was relevant for the observed TMBIM4-dependent increase in cell survival.

Analysis after the first four days showed that the viability of all the cells form all three cell lines was maintained. However, after 14 days of starvation conditions, only TMBIM4 overexpression cell line remained with a cell viability close to 100% (unpublish data) (Figure 21, PBS condition). Figure 21 shows that TMBIM4 overexpression cell line endured starvation culture conditions better than the rest, surviving for longer periods of time, meaning that increased TMBIM4 expression protects OS cells. The phenotype was identified as cell death after 14 days under starvation conditions. To check if this TMBIM4-dependent phenotype is dependent on the ability of TMBIM4 to increase H_2O_2 cell concentrations, these were altered by addition of catalase or H_2O_2 as described before, since overexpression of TMBIM4 leads to an increase of H_2O_2 inside the cell. The results can be seen in figure 21, and they suggest that the increase or reduction in H_2O_2 concentration did not make cells more or less resistant to cell death after long periods in culture. Simultaneously, CAT, an enzyme that degrades H_2O_2, was tested and, once again, no changes were observed in the phenotype as cell and nucleus morphology remained unchanged by treatment with both H_2O_2 and CAT (figure 21). This way, it is suggested that H_2O_2 does not play an important role in this phenotype. Figure 21 also shows a minor increase in toxicity, as can be seen by the slight greater cell death. Results regarding flow cytometry analysis of sub-G1 cell cycle phase are currently being analysed by our group as well as more tests are being carried out.

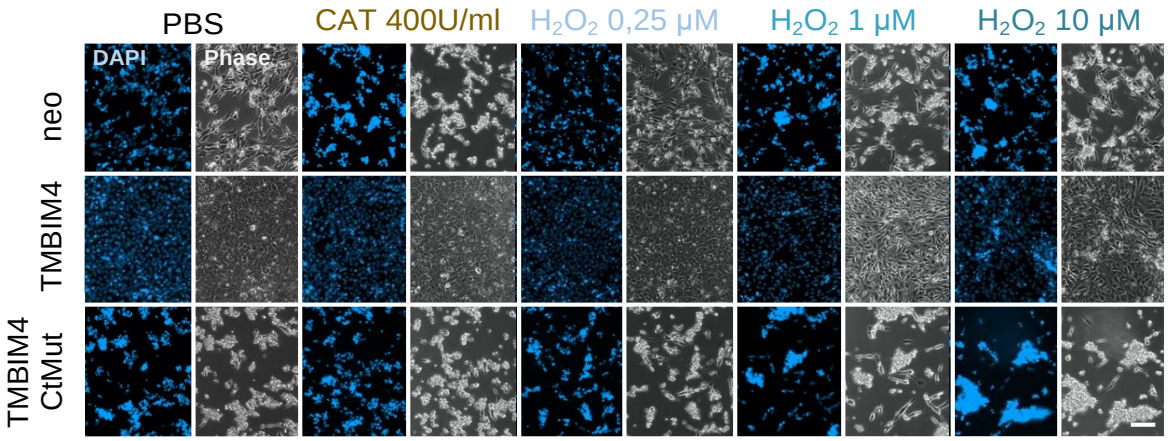

Figure 21 *– Fluorescence and phase contract images showing U2OS cell line with fluorescent marker DAPI staining the nucleus in blue and the cell morphology in the various conditions of the assay. Cells were kept in culture for 14 days without media changes in the presence of the indicated compounds. Scale bar of 200 µm. Representative image of 3 experiments, where results remained the same across experiments.*

Conclusion

Non-published bioinformatic data from our group states that the higher the stage of the glioma tumour, the greater TMBIM4 expression in those tumours. Regarding this statement it was of interest to observe that when this protein is highly expressed, there is an impact on the cancer patient survival, suggesting that it is important for glioma progression (TCGA data). The protocols and results obtained during this project will allow the further exploration of the impact of the overexpression of TMBIM4 on several glioma cell biology processes that are relevant for cancer progression and the dissection of the role of TMBIM4 in those processes. The data obtained will allow to evaluate the impact of TMBIM4 on the TMZ resistance of GB cells. The next step in this work will be to closely mimic the current treatment protocol in a 3D biology cell culture model, including RT and CT therapy, to assess if TMBIM4 silencing has the same effects in the closest to reality *in vitro* model available. This assay is currently being performed by our group in collaboration with another group.

With the silencing of TMBIM4 there was a reduction in motility (migration and invasion) of glioma cancer cells; ideally, we will investigate if with the overexpression of this protein, the opposite effect occurs, that is, if there is an increase in motility the higher the expression. Regarding the importance of TMBIM4 for osteosarcoma, the findings conveyed in this work support that H_2O_2 is not the reason behind the observed TMBIM4 overexpression-dependent increase in cell survival under starvation conditions. Future experiments are planned to explore the role of *de novo* cysteine synthesis in the TMBIM-dependent phenotype. The production of cysteine through the transsulfuration pathway is essential for the progression of several cancers as it may provide several elements essential for cellular proliferation and survival (Bonifácio et al., 2021; Ruiz-Rodado et al., 2022). This is relevant as cancer cells counteract the increase of ROS such as H_2O_2 through antioxidant protection, and cysteine takes on a very important role in this redox stability, so much so that studies have showed that compromising the equilibrium of the transsulfuration pathway seems to reduce tumour growth *in vivo*, becoming a hopeful strategy to induce death in tumour cells (Daher et al., 2020; Zhu et al., 2019).

Other TMBIM proteins have also showed impact on cancer progression. For example, TMBIM6, similarly to TMBIM4, was found to be frequently overexpressed in many different cancers and its knockdown further diminishes tumour development (Kim et al., 2020). The tumours with high levels of TMBIM6 had a worse prognosis regardless of the type of cancer. This protein was also associated with promotion of the metastasis process through motility of cells and their invasiveness, and regulates glucose

metabolism by opposition to TMBIM4, which is related to Ca^{2+} metabolism (Kim et al., 2020). Specifically in GBM, TMBIM1 is another protein found to be overexpressed (Cai et al., 2022). Studies done on U87 and U251 cells indicate that this protein decreases apoptosis and stimulates resistance to TMZ (Cai et al., 2022). TMBIM1 expression reduction reduces cells viability which is not the case for TMBIM4. The same study showed that a TMBIM1 knockdown group had a significant increase in survival time in an *in vivo* experiment done on mice (Cai et al., 2022). This way, the results present in literature combined with our data further establish the potential and role of the TMBIM protein family in future cancer therapy.

The hypotheses here presented are currently being explored and further investigated by our group to better understand the impact of TMBIM4 expression dysregulation in the context of cancer progression-associated cellular processes. This is relevant in cancers with high mortality rates such as glioma and OS, with the goal of contributing to the development of alternative therapeutical approaches by making tumours more susceptible to therapy or by defining new markers for prognosis.

References

Absher, M. (1973). Hemocytometer Counting. *Tissue Culture*, 395–397. https://doi.org/10.1016/B978-0-12-427150-0.50098-X

Almeida, N., Carrara, G., Palmeira, C. M., Fernandes, A. S., Parsons, M., Smith, G. L., & Saraiva, N. (2020). Stimulation of cell invasion by the Golgi Ion Channel GAAP/TMBIM4 via an H 2 O 2-Dependent Mechanism. *Redox Biology*, *28*. https://doi.org/10.1016/J.REDOX.2019.101361

Barbedo, J. (2013). Automatic Object Counting In Neubauer Chambers. *Anais de XXXI Simpósio Brasileiro de Telecomunicações*. https://doi.org/10.14209/sbrt.2013.34

Bonifácio, V. D. B., Pereira, S. A., Serpa, J., & Vicente, J. B. (2021). Cysteine metabolic circuitries: druggable targets in cancer. In *British Journal of Cancer* (Vol. 124, Issue 5, pp. 862–879). Springer Nature. https://doi.org/10.1038/s41416-020-01156-1

Cai, J., Gao, L., Wang, Y., Li, Y., Ye, Z., Tong, S., Yan, T., sun, Q., Xu, Y., Jiang, H., Zhang, S., Zhao, L., Yang, J., & Chen, Q. (2022). TMBIM1 promotes proliferation and attenuates apoptosis in glioblastoma cells by targeting the p38 MAPK signalling pathway. *Translational Oncology*, *19*. https://doi.org/10.1016/j.tranon.2022.101391

Carrara, G., Parsons, M., Saraiva, N., & Smith, G. L. (2017). Golgi anti-apoptotic protein: A tale of camels, calcium, channels and cancer. *Open Biology*, *7*(5). https://doi.org/10.1098/rsob.170045

Chen, C., Xie, L., Ren, T., Huang, Y., Xu, J., & Guo, W. (2021). Immunotherapy for osteosarcoma: Fundamental mechanism, rationale, and recent breakthroughs. In *Cancer Letters* (Vol. 500, pp. 1–10). Elsevier Ireland Ltd. https://doi.org/10.1016/j.canlet.2020.12.024

Chen, R., Smith-Cohn, M., Cohen, A. L., & Colman, H. (2017). Glioma Subclassifications and Their Clinical Significance. *Neurotherapeutics : The Journal of the American Society for Experimental NeuroTherapeutics*, *14*(2), 284–297. https://doi.org/10.1007/S13311-017-0519-X

Cortamp, I., June-Koo Lee, J., Xi, R., Jain, D., Jung, Y. L., Yang, L., Gordenin, D., Klimczak, L. J., Zhang, C.-Z., Pellman, D. S., Akdemir, K. C., Alvarez, E. G., Baez-Ortega, A., Beroukhim, R., Boutros, P. C., L Bowtell, D. D., Brors, B., Burns, K. H., Campbell, P. J., … von Mering, C. (2020). Comprehensive analysis of chromothripsis in 2,658 human cancers using whole-genome sequencing. *Nature Genetics 2020 52:3*, *52*(3), 331–341. https://doi.org/10.1038/s41588-019-0576-7

Daher, B., Vučetić, M., & Pouysségur, J. (2020). Cysteine Depletion, a Key Action to Challenge Cancer Cells to Ferroptotic Cell Death. In *Frontiers in Oncology* (Vol. 10). Frontiers Media S.A. https://doi.org/10.3389/fonc.2020.00723

Davis, M. E. (2018). Epidemiology and Overview of Gliomas. In *Seminars in Oncology Nursing* (Vol. 34, Issue 5, pp. 420–429). W.B. Saunders. https://doi.org/10.1016/j.soncn.2018.10.001

Delgado-López, P. D., Saiz-López, P., Gargini, R., Sola-Vendrell, E., & Tejada, S. (2020). A comprehensive overview on the molecular biology of human glioma: what the clinician needs to know. In *Clinical and Translational Oncology* (Vol. 22, Issue 11, pp. 1909–1922). Springer Science and Business Media Deutschland GmbH. https://doi.org/10.1007/s12094-020-02340-8

Gill, J., & Gorlick, R. (2021). Advancing therapy for osteosarcoma. In *Nature Reviews Clinical Oncology* (Vol. 18, Issue 10, pp. 609–624). Nature Research. https://doi.org/10.1038/s41571-021-00519-8

Gubser, C., Bergamaschi, D., Hollinshead, M., Lu, X., Kuppeveld, F. J. M. Van, & Smith, G. L. (2007). A new inhibitor of apoptosis from vaccinia virus and eukaryotes. *PLoS Pathogens*, *3*(2), 246–259. https://doi.org/10.1371/JOURNAL.PPAT.0030017

Gubser, C., Bergamaschi, D., Hollinshead, M., Lu, X., Van Kuppeveld, F. J. M., & Smith, G. L. (2007). A new inhibitor of apoptosis from vaccinia virus and eukaryotes. *PLoS Pathogens*, *3*(2), 246–259. https://doi.org/10.1371/JOURNAL.PPAT.0030017

Gusyatiner, O., & Hegi, M. E. (2018). Glioma epigenetics: From subclassification to novel treatment options. *Seminars in Cancer Biology*, *51*, 50–58. https://doi.org/10.1016/J.SEMCANCER.2017.11.010

Harada, S., Wei, S., & Siegal, G. P. (2015). Molecular pathology of osteosarcoma. *Bone Cancer: Primary Bone Cancers and Bone Metastases: Second Edition*, 213–222. https://doi.org/10.1016/B978-0-12-416721-6.00019-4

Jiapaer, S., Furuta, T., Tanaka, S., Kitabayashi, T., & Nakada, M. (2018). Potential strategies overcoming the temozolomide resistance for glioblastoma. *Neurologia Medico-Chirurgica*, *58*(10), 405–421. https://doi.org/10.2176/nmc.ra.2018-0141

Kim, H. K., Bhattarai, K. R., Junjappa, R. P., Ahn, J. H., Pagire, S. H., Yoo, H. J., Han, J., Lee, D., Kim, K. W., Kim, H. R., & Chae, H. J. (2020). TMBIM6/BI-1 contributes to cancer progression through assembly with mTORC2 and AKT activation. *Nature Communications*, *11*(1). https://doi.org/10.1038/s41467-020-17802-4

Li, T., Li, J., Chen, Z., Zhang, S., Li, S., Wageh, S., Al-Hartomy, O. A., Al-Sehemi, A. G., Xie, Z., Kankala, R. K., & Zhang, H. (2022). Glioma diagnosis and therapy: Current challenges and nanomaterial-based solutions. In *Journal of Controlled Release* (Vol. 352, pp. 338–370). Elsevier B.V. https://doi.org/10.1016/j.jconrel.2022.09.065

Liu, S., Shi, W., Zhao, Q., Zheng, Z., Liu, Z., Meng, L., Dong, L., & Jiang, X. (2021). Progress and prospect in tumor treating fields treatment of glioblastoma. *Biomedicine & Pharmacotherapy = Biomedecine & Pharmacotherapie*, *141*. https://doi.org/10.1016/J.BIOPHA.2021.111810

Ma, R., Taphoorn, M. J. B., & Plaha, P. (2021). Advances in the management of glioblastoma. In *Journal of Neurology, Neurosurgery and Psychiatry* (Vol. 92, Issue 10, pp. 1103–1111). BMJ Publishing Group. https://doi.org/10.1136/jnnp-2020-325334

National Cancer Institute. (2023). *Bone and Joint Cancer — Cancer Stat Facts*. NIH. https://seer.cancer.gov/statfacts/html/bones.html

NHI. (2023, August 13). *Stem Cell Basics*. https://stemcells.nih.gov/info/basics/stc-basics

Nirala, B. K., Yamamichi, T., & Yustein, J. T. (2023). Deciphering the Signaling Mechanisms of Osteosarcoma Tumorigenesis. In *International Journal of Molecular Sciences* (Vol. 24, Issue 14). Multidisciplinary Digital Publishing Institute (MDPI). https://doi.org/10.3390/ijms241411367

Ortiz, R., Perazzoli, G., Cabeza, L., Jiménez-Luna, C., Luque, R., Prados, J., & Melguizo, C. (2020). Temozolomide: An Updated Overview of Resistance Mechanisms, Nanotechnology Advances and Clinical Applications. *Current Neuropharmacology*, *19*(4), 513–537. https://doi.org/10.2174/1570159x18666200626204005

Ostrom, Q. T., Bauchet, L., Davis, F. G., Deltour, I., Fisher, J. L., Langer, C. E., Pekmezci, M., Schwartzbaum, J. A., Turner, M. C., Walsh, K. M., Wrensch, M. R., & Barnholtz-Sloan, J. S. (2014). The epidemiology of glioma in adults: A state of the science review. *Neuro-Oncology*, *16*(7), 896–913. https://doi.org/10.1093/neuonc/nou087

Ou, A., Alfred Yung, W. K., & Majd, N. (2021). Molecular mechanisms of treatment resistance in glioblastoma. In *International Journal of Molecular Sciences* (Vol. 22, Issue 1, pp. 1–24). MDPI AG. https://doi.org/10.3390/ijms22010351

Präbst, K., Engelhardt, H., Ringgeler, S., & Hübner, H. (2017). Basic colorimetric proliferation assays: MTT, WST, and resazurin. In *Methods in Molecular Biology* (Vol. 1601, pp. 1–17). Humana Press Inc. https://doi.org/10.1007/978-1-4939-6960-9_1

Qin, Z., Liang, W., Zhang, Z., Li, P., Wang, T., Chen, Q., Guo, B., Zhong, Y., Kang, H., & Wang, L. (2023). Activated KRAS reprograms neural progenitor cells to glioma stem cell-like phenotype. *International Journal of Oncology*, *63*(1). https://doi.org/10.3892/ijo.2023.5536

Reuss, D. E., Downing, S. M., Camacho, C. V., Wang, Y. D., Piro, R. M., Herold-Mende, C., Wang, Z. Q., Hofmann, T. G., Sahm, F., von Deimling, A., McKinnon, P. J., & Frappart, P. O. (2023). Simultaneous Nbs1 and p53 inactivation in neural progenitors triggers high-grade gliomas. *Neuropathology and Applied Neurobiology*, *49*(4). https://doi.org/10.1111/nan.12915

Rojas-Rivera, D., & Hetz, C. (2015). TMBIM protein family: ancestral regulators of cell death. *Oncogene*, *34*(3), 269–280. https://doi.org/10.1038/ONC.2014.6

Ruiz-Rodado, V., Dowdy, T., Lita, A., Kramp, T., Zhang, M., Jung, J., Dios-Esponera, A., Zhang, L., Herold-Mende, C. C., Camphausen, K., Gilbert, M. R., & Larion, M. (2022). Cysteine is a limiting factor for glioma proliferation and survival. *Molecular Oncology*, *16*(9), 1777–1794. https://doi.org/10.1002/1878-0261.13148

Santos, K. R., & Mariano, A. B. (2014). Determination of Optimal Algae Concentration for Continuous Growth of Scenedesmus sp. in Chu and Modified Media. *Revista de Engenharia Térmica*, *13*(2), 52. https://doi.org/10.5380/reterm.v13i2.62096

Saraiva, N., Prole, D. L., Carrara, G., Johnson, B. F., Taylor, C. W., Parsons, M., & Smith, G. L. (2013). hGAAP promotes cell adhesion and migration via the stimulation of store-operated Ca2+ entry and calpain 2. *The Journal of Cell Biology*, *202*(4), 699–713. https://doi.org/10.1083/JCB.201301016

Sularsih, S., Soetjipto, S., & Rahayu, R. P. (2019). Cytotoxicity of Combination Chitosan with Different Molecular Weight and Ethanol Extracted Aloe vera using MTT Assay. *IOP Conference Series: Earth and Environmental Science*, *217*(1). https://doi.org/10.1088/1755-1315/217/1/012030

Swift, L. H., & Golsteyn, R. M. (2016). The Relationship Between Checkpoint Adaptation and Mitotic Catastrophe in Genomic Changes in Cancer Cells. *Genome Stability:*

From Virus to Human Application, 373–389. https://doi.org/10.1016/B978-0-12-803309-8.00022-7

Weller, M., van den Bent, M., Preusser, M., Le Rhun, E., Tonn, J. C., Minniti, G., Bendszus, M., Balana, C., Chinot, O., Dirven, L., French, P., Hegi, M. E., Jakola, A. S., Platten, M., Roth, P., Rudà, R., Short, S., Smits, M., Taphoorn, M. J. B., … Wick, W. (2021). EANO guidelines on the diagnosis and treatment of diffuse gliomas of adulthood. *Nature Reviews Clinical Oncology*, *18*(3), 170–186. https://doi.org/10.1038/s41571-020-00447-z

WHO. (2023). *Global Cancer Observatory*. https://gco.iarc.fr/

Xu, S., Tang, L., Li, X., Fan, F., & Liu, Z. (2020). Immunotherapy for glioma: Current management and future application. In *Cancer Letters* (Vol. 476, pp. 1–12). Elsevier Ireland Ltd. https://doi.org/10.1016/j.canlet.2020.02.002

Zhang, C., Liu, J., Xu, D., Zhang, T., Hu, W., & Feng, Z. (2020). Gain-of-function mutant p53 in cancer progression and therapy. *Journal of Molecular Cell Biology*, *12*(9), 674–687. https://doi.org/10.1093/JMCB/MJAA040

Zhang, H. F., Klein Geltink, R. I., Parker, S. J., & Sorensen, P. H. (2022). Transsulfuration, minor player or crucial for cysteine homeostasis in cancer. In *Trends in Cell Biology* (Vol. 32, Issue 9, pp. 800–814). Elsevier Ltd. https://doi.org/10.1016/j.tcb.2022.02.009

Zhang, W., Lv, Y., Xue, Y., Wu, C., Yao, K., Zhang, C., Jin, Q., Huang, R., Li, J., Sun, Y., Su, X., Jiang, T., & Fan, X. (2016). *Co-expression modules of NF1, PTEN and sprouty enable distinction of adult diffuse gliomas according to pathway activities of receptor tyrosine kinases*. *7*(37). www.impactjournals.com/oncotarget

Zhu, J., Berisa, M., Schwörer, S., Qin, W., Cross, J. R., & Thompson, C. B. (2019). Transsulfuration Activity Can Support Cell Growth upon Extracellular Cysteine Limitation. *Cell Metabolism*, *30*(5), 865-876.e5. https://doi.org/10.1016/j.cmet.2019.09.009